

I. SURFACE DEFORMATIONS IN A DRAINING
CYLINDRICAL TANK

II. STABILITY OF A LAMINAR FILM
ON AN INCLINED PLANE

Thesis by
Franklin Lester Marshall

In Partial Fulfillment of the Requirements
For the Degree of
Doctor of Philosophy

California Institute of Technology
Pasadena, California

1967

(Submitted December 8, 1966)

ACKNOWLEDGMENTS

The author wishes to express his deepest gratitude to Professor W. D. Rannie for his ever-available blackboard and the many hours in front of same devoted to enlightening discussions and the offering of vital suggestions and encouragement, without all of which this thesis would not have been possible.

The author also wishes to thank Mrs. Roberta Duffy for the accurate and efficient typing of these pages.

In addition, the author acknowledges the financial support provided by fellowships from the National Aeronautics and Space Administration and the Ford Foundation.

ABSTRACT

I. The problem of draining of a liquid from a cylindrical tank through a hole in the bottom is considered. The flow is irrotational, and the free surface boundary conditions are linearized. Solutions are obtained and the shape of the free surface determined for any constant mass flow rate. At large mass flow rates, the free surface deforms appreciably when the mean depth is about 40 per cent or less of the tank diameter.

The initial acceleration distribution of the free surface and the transient behavior of the mass flow rate are determined for a flow started impulsively from rest as a result of a constant pressure head.

At large Froude numbers it is possible to compare the results with the recent experiments of Gluck, Gille, Zukoski, and Simkin, and the present analysis is consistent with the experimental observations.

II. The stability characteristics of a laminar film with a free surface flowing under the action of gravity down an inclined plane are examined. Approximate solutions of the Orr-Sommerfeld equation are obtained. These are valid as long as the wave speed of the disturbance is somewhat larger than the maximum velocity of the undisturbed flow. Curves of neutral stability as functions of Reynolds number of the undisturbed flow and wave number of the disturbance are found. These are valid over a larger domain of Reynolds num-

ber and wave number than the previous results of Benjamin.

The special case of a vertical wall and zero surface tension is also discussed. It is shown that undamped waves of the type predicted by Yih (and tentatively suggested by Benjamin) cannot exist, and a source of error in Yih's analysis is suggested.

TABLE OF CONTENTS

<u>Part</u>	<u>Title</u>	<u>Page</u>
	Acknowledgments	ii
	Abstract	iii
	Table of Contents	v
I.	<u>Surface Deformation in a Draining Cylindrical Tank</u>	1
	1.1 Introduction	2
	1.2 Statement of the Problem	4
	1.3 Notation	5
	1.4 Formulation	6
	1.5 Zeroth-order Flow	9
	1.6 First-order Flow	11
	1.7 Initial Accelerations	21
	1.8 Zeroth-order Starting Transient	28
	1.9 Concluding Remarks	32
II.	<u>Stability of a Laminar Film on an Inclined Plane</u>	35
	2.1 Introduction	36
	2.2 Notation	41
	2.3 Formulation	44
	2.4 Review of Past Attempts to Solve the Problem	54
	2.5 The Present Solution	59
	2.6 Energy Conservation	64
	2.7 The Case of a Vertical Wall and a Liquid Without Surface Tension	66
	2.8 Concluding Remarks	71
	Figures	72
	References	86

PART I. SURFACE DEFORMATIONS IN A
DRAINING CYLINDRICAL TANK

1.1 Introduction

Until very recently, there has been very little attention focused on the problem of the irrotational draining of a liquid from a tank, since vortex formation usually plays a dominant role, particularly with respect to the deformation of the free surface. However, at very large mass flow rates, such as may be produced under the action of a pressure head many times greater than the normal gravitational head, rotational effects become unimportant (unless, of course, they are artificially enhanced by external means), but large surface deformations can occur nevertheless.

In modern liquid-propellant rockets, propellant tanks are often drained at extremely large flow rates, and the resulting surface deformations can lead to the ingestion of pressurization gas into the drain hole well before all the propellant has been emptied from the tank. As a consequence, there has been renewed interest in studying the phenomena involved.

The problem of irrotational flow from a cylindrical tank was treated by Saad and Oliver¹⁵ in 1964 for the case of a constant mass flow rate. As will be shown, however, their analysis contains a serious error which renders their result invalid except in the case of small Froude numbers. (The Froude number, which may be taken in this problem as a nondimensional measure of the mass flow rate, is defined as the ratio of the time rate of change of the mean surface height to the square root of the product of the cylinder radius and the acceleration due to gravity.) Even without this error, their solution is based on approximations which are valid only in the case in which,

first of all, the Froude number is small compared to the ratio of the cylinder radius to the exit hole radius and, secondly, the displacement of the mean surface height from its starting position is small compared to the cylinder radius. But it is precisely the case of large Froude numbers and large distances of travel from the starting position of the mean surface height that is of primary importance; hence it is desirable to have a method of solution which is valid under these conditions.

Such a method is presented here. For the case of a constant mass flow rate the surface profiles are found, and the accuracy of the solution is seen to be independent of the size of the Froude number or the distance traveled by the mean surface height. Instead, it is assumed that the mean surface height itself is not small (i.e., not less than about one fourth of the tank diameter). It is found that in the limit of very large Froude number F the shape of the surface is independent of F , and for small F the amplitude of the surface deformation is proportional to F^2 . (Hence this phenomenon is not easily observed in one's kitchen sink; any visible deformations are most likely due to the presence of a vortex.) At low starting heights and low Froude numbers, surface oscillations, originally predicted by Saad and Oliver, are found; it is argued here, however, that these oscillations are largely the result of boundary conditions (both in the treatment of Saad and Oliver and here) which become unrealistic in the case of low starting heights. The starting transient (for which the net pressure head, rather than the mass flow rate, is held constant) is also examined, and the results give some insight into

the nature of the surface deformation phenomenon.

1.2 Statement of the Problem

The flow field considered is that of an incompressible fluid draining from a tank which is in the shape of a right circular cylinder of radius a with its axis parallel to the gravity field (see Figure 1). The fluid leaves the cylinder through a circular hole of radius $a\delta$ in the center of the plane bottom. The center of the hole is taken as the origin of the coordinate system, with the positive z -axis pointing to the interior of the cylinder in the direction opposite to that of the gravity field. The upper surface of the liquid is free and is characterized by a coefficient of surface tension σ . The flow is assumed to be irrotational at all points and axially symmetric.

The liquid is considered to be draining under the combined action of gravity and a net pressure head, but it will be assumed that the rate of mass flow out of the cylinder is constant. (This implies that the pressure head varies in a precise way with time, but this is not unrealistic; constant mass flow rates are often required in propellant tank applications.) The initial conditions are that the surface is undeformed (i. e., in a horizontal plane) and all points in the surface have initially the same z -component of velocity. Thus, in effect, the fluid is assumed to have been draining at a constant rate with the surface constrained to be in a horizontal plane, and at the initial instant the constraint is removed and the surface becomes free. (The question of how realistic the assumed initial conditions are, will be treated later.)

1.3 Notation

The following symbols will be used to represent dimensional parameters (refer to Figure 1):

a = radius of the cylinder

g = acceleration due to gravity (and, possibly, due to an axial acceleration of the cylindrical tank)

h = average height of the surface above the bottom

p^* = pressure

r = radial coordinate

R_1 = radius of curvature of the surface in radial direction

R_2 = radius of curvature of the surface in the azimuthal direction

t^* = time

$U = - \frac{dh}{dt^*}$ = rate at which average surface height decreases (a positive constant)

z^* = axial coordinate

ρ = density

σ = coefficient of surface tension

ϕ^* = velocity potential (the sign convention used is that the velocity field is the positive gradient of the potential function)

The following symbols will be used to represent nondimensional parameters:

$$A_n = \frac{2}{\lambda_n^2 \delta} \frac{J_1(\lambda_n \delta)}{[J_0(\lambda_n)]^2}$$

$$B = \frac{\rho g a^2}{\sigma} = \text{Bond number}$$

$B_n = n^{\text{th}}$ coefficient of series for first-order potential function

$$F = \frac{U}{\sqrt{ag}} = \text{Froude number}$$

$$J_i = \text{Bessel function of the first kind of order } i$$

$$\rho = \frac{\rho^*}{\rho U^2}$$

$$t = \frac{t^*}{a/U}$$

$$z = \frac{z^*}{a}$$

$$\delta = \text{ratio of exit hole radius to cylinder radius}$$

$$\xi = \text{ratio of local displacement of surface (from mean value) to cylinder radius}$$

$$\eta = \frac{r}{a}$$

$$\lambda_n = n^{\text{th}} \text{ zero of } J_1 \text{ (} J_1(\lambda_n) = 0 \text{)}$$

$$\xi = \frac{h}{a}$$

$$\xi_0 = \text{initial value of } \xi$$

$$\phi = \frac{\phi^*}{Ua}$$

$$\phi_0 = \text{zeroth-order part of } \phi$$

$$\phi_1 = \text{first-order part of } \phi$$

$$\omega_n = \frac{1}{F} \sqrt{\lambda_n \left(1 + \frac{\lambda_n^2}{B} \right)}$$

1.4 Formulation

Since the flow is irrotational and axially symmetric, we seek a velocity potential ϕ which satisfies the following form of Laplace's equation:

$$\frac{1}{\eta} \frac{\partial}{\partial \eta} \left(\eta \frac{\partial \phi}{\partial \eta} \right) + \frac{\partial^2 \phi}{\partial z^2} = 0 \quad (1.1)$$

On the cylinder axis and the outer wall, respectively, the following boundary conditions apply:

$$(I) \quad \left. \frac{\partial \phi}{\partial \eta} \right|_{\eta=0} = 0, \quad (1.2)$$

$$(II) \quad \left. \frac{\partial \phi}{\partial \eta} \right|_{\eta=1} = 0 \quad (1.3)$$

It will be assumed that the flow through the exit hole is adequately described by requiring the z -component of velocity to be uniformly distributed across the hole in the plane of the bottom. Thus, the boundary condition at the bottom becomes:

$$(III) \quad \left. \frac{\partial \phi}{\partial z} \right|_{z=0} = \begin{cases} -\frac{1}{\delta^2} & \text{for } 0 \leq \eta < \delta \\ 0 & \text{for } \delta \leq \eta \leq 1 \end{cases} \quad (1.4)$$

At the free surface, as is usually the case with free surface flows, two boundary conditions are required. This arises from the fact that the location of the boundary is unknown, i. e., $\mathfrak{F} = \mathfrak{F}(\eta, t)$ is an unknown function. One of these conditions is a kinematic relation which guarantees that the function $\mathfrak{F}(\eta, t)$ is consistent with the potential function, that is, that fluid particles in the surface remain in the surface. In dimensional form we have:

$$(IV) \quad \frac{\partial(h+a\mathfrak{F})}{\partial t^*} = \left[\frac{\partial \phi^*}{\partial z^*} \right]_{z^*=h+a\mathfrak{F}} - \frac{\partial(h+a\mathfrak{F})}{\partial r} \left[\frac{\partial \phi^*}{\partial r} \right]_{z^*=h+a\mathfrak{F}} \quad (1.5)$$

The other free surface boundary condition is the dynamical relation which actually governs the motion of the free surface. It is Bernoulli's integral of the equations of motion evaluated at the surface, which in dimensional notation becomes:

$$(V) \left[\frac{p^*}{\rho} + \frac{1}{2} \left(\frac{\partial \phi^*}{\partial z^*} \right)^2 + \frac{1}{2} \left(\frac{\partial \phi^*}{\partial r} \right)^2 + g z^* + \frac{\partial \phi^*}{\partial t^*} \right]_{z=h+a\mathfrak{f}} = f_1(t^*) \quad , \quad (1.6)$$

where $f_1(t^*)$ is a function of t^* only.

Before nondimensionalizing equations (1.5) and (1.6), we note the following. First of all, we may choose the pressure above the surface as the zero of the pressure scale without loss of generality, in which case the pressure in the liquid at the surface is just that due to surface tension effects:

$$p^* \Big|_{z=h+a\mathfrak{f}} = -\sigma \left(\frac{1}{R_1} + \frac{1}{R_2} \right) \quad , \quad (1.7)$$

where R_1 is the radius of curvature of the surface in the radial direction and R_2 , the radius of curvature in the azimuthal direction. Since the problem is going to be linearized with respect to \mathfrak{f} , we may write R_1 and R_2 in the following way:

$$\frac{1}{R_1} = \frac{\partial^2 (h+a\mathfrak{f})}{\partial r^2} + O(\mathfrak{f}^3) \quad , \quad (1.8a)$$

$$\frac{1}{R_2} = \frac{1}{r} \frac{\partial (h+a\mathfrak{f})}{\partial r} + O(\mathfrak{f}^3) \quad . \quad (1.8b)$$

In addition, we note that there will be no explicit time dependence in the problem; all variations with respect to time are implied by functions of h , since h is a function of time. It is therefore convenient to use h (or \mathfrak{f}) as the independent variable which reflects time variations. We note that

$$\frac{\partial}{\partial t^*} = \frac{\partial h}{\partial t^*} \frac{\partial}{\partial h} \quad \text{or} \quad \frac{\partial}{\partial t} = - \frac{\partial}{\partial \mathfrak{f}}$$

Thus, the nondimensional forms of equations (1.5) and (1.6) become:

$$(IV) \quad \frac{\partial \mathfrak{f}}{\partial \mathfrak{z}} = -1 - \left[\frac{\partial \phi}{\partial \mathfrak{z}} \right]_{\mathfrak{z}=\mathfrak{z}+\mathfrak{f}} + \frac{\partial \mathfrak{f}}{\partial \eta} \left[\frac{\partial \phi}{\partial \eta} \right]_{\mathfrak{z}=\mathfrak{z}+\mathfrak{f}}, \quad (1.9)$$

$$(V) \quad -\frac{1}{\mathfrak{B}F^2} \frac{1}{\eta} \frac{\partial}{\partial \eta} \left(\eta \frac{\partial \mathfrak{f}}{\partial \eta} \right) + \frac{\mathfrak{f}}{F^2} + \left[\frac{1}{2} \left(\frac{\partial \phi}{\partial \mathfrak{z}} \right)^2 + \frac{1}{2} \left(\frac{\partial \phi}{\partial \eta} \right)^2 - \frac{\partial \phi}{\partial \mathfrak{z}} \right]_{\mathfrak{z}=\mathfrak{z}+\mathfrak{f}} = f_2(\mathfrak{f}), \quad (1.10)$$

where \mathfrak{B} is the Bond number $\frac{\rho g a^2}{\sigma}$ and F is the Froude number $U/\sqrt{a g}$. The function $f_2(\mathfrak{f})$ is a function of \mathfrak{f} only, that is to say, it is not a function of η or \mathfrak{z} .

Thus we seek a solution to equation (1.1) satisfying boundary conditions (I) through (V). The approach to be used is to assume that \mathfrak{f} is small compared to one and to linearize the equations with respect to \mathfrak{f} . We expand ϕ in the following way:

$$\phi = \phi_0 + \phi_1 + \dots, \quad (1.11)$$

in which we define ϕ_0 to be the potential function for the flow field in the absence of surface deformations; this will be called the zeroth-order flow. Similarly, ϕ_1 gives the first-order correction to ϕ_0 obtained by keeping terms of order \mathfrak{f} only, dropping higher order terms. The flow field generated by the sum of ϕ_0 and ϕ_1 will be called the first-order flow.

1.5 Zeroth-order Flow

Taking the zeroth-order part of equation (1.1), we find

$$\frac{1}{\eta} \frac{\partial}{\partial \eta} \left(\eta \frac{\partial \phi_0}{\partial \eta} \right) + \frac{\partial^2 \phi_0}{\partial \mathfrak{z}^2} = 0 \quad (1.12)$$

The zeroth-order parts of boundary conditions (I), (II), and (III) become

$$(I) \quad \left. \frac{\partial \phi_0}{\partial \eta} \right|_{\eta=0} = 0, \quad (1.13)$$

$$(II) \quad \left. \frac{\partial \phi_0}{\partial \eta} \right|_{\eta=1} = 0, \quad (1.14)$$

$$(III) \quad \left. \frac{\partial \phi_0}{\partial \eta} \right|_{\eta=0} = \begin{cases} -\frac{1}{\delta} & \text{for } 0 \leq \eta < \delta \\ 0 & \text{for } \delta \leq \eta \leq 1 \end{cases} \quad (1.15)$$

Since the zeroth-order flow corresponds, by definition, to a surface constrained to remain in a horizontal plane, the free surface boundary conditions (IV) and (V) are clearly not the ones to use. Instead, we need merely to require that the surface moves downward with a speed U ; in nondimensional notation that becomes

$$\left. \frac{\partial \phi_0}{\partial \eta} \right|_{\eta=\xi} = -1. \quad (1.16)$$

The solution to equation (1.12) satisfying conditions (1.13), (1.14), (1.15), and (1.16) is seen to be

$$\phi_0 = -\eta + \sum_{n=1}^{\infty} A_n \frac{\cosh \lambda_n (\eta - \xi)}{\sinh \lambda_n \xi} J_0(\lambda_n \eta), \quad (1.17a)$$

where λ_n is the n^{th} root of $J_1(\lambda_n) = 0$, and

$$A_n = \frac{2}{\lambda_n^2 \delta} \frac{J_1(\lambda_n \delta)}{[J_0(\lambda_n)]^2}. \quad (1.17b)$$

J_0 and J_1 are Bessel functions of the first kind of order zero and one, respectively.

We note for future reference that A_n is of order one and is a decreasing function of n . Also, for increasing n , we see that the quantity $[\cosh \lambda_n(z-f)] / \sinh \lambda_n f$ decreases roughly like $e^{-\lambda_n f}$ if z is near f . Thus, if z is not too small, the series in equation (1.17a) is a rapidly converging one, and may be accurately represented by a finite truncation.

1.6 First-Order Flow

The initial conditions assumed for the first-order flow are that there is no deformation of the surface, and that all points in the surface have the same z -component of velocity ($= U$). Thus,

$$\eta \Big|_{f=f_0} = 0, \quad (1.18)$$

and

$$\frac{\partial \eta}{\partial f} \Big|_{f=f_0} = 0. \quad (1.19)$$

The first-order part of equation (1.1) is

$$\frac{1}{\eta} \frac{\partial}{\partial \eta} \left(\eta \frac{\partial \phi_1}{\partial \eta} \right) + \frac{\partial^2 \phi_1}{\partial z^2} = 0 \quad (1.20)$$

Similarly, the boundary conditions (I), (II), and (III) become, for ϕ_1 ,

$$(I) \quad \frac{\partial \phi_1}{\partial \eta} \Big|_{\eta=0} = 0 \quad (1.21)$$

$$(II) \quad \frac{\partial \phi_1}{\partial \eta} \Big|_{\eta=1} = 0 \quad (1.22)$$

$$(III) \quad \left. \frac{\partial \Phi}{\partial g} \right|_{g=0} = 0 \quad (1.23)$$

The most general solution to equation (1.20) which satisfies conditions (I), (II), and (III) is:

$$\Phi = \sum_{n=1}^{\infty} B_n(\xi) \cosh \lambda_n g J_0(\lambda_n \eta) \quad (1.24)$$

where the B_n 's are arbitrary functions of ξ . (The "most general" solution would include an additional function of ξ , say $B_0(\xi)$, but such a function can clearly be ignored without loss of generality in the present problem.)

For the present it will be assumed that the series in equation (1.24) is rapidly convergent; this assumption may be checked after the functions $B_n(\xi)$ are found. On this basis, we shall truncate the series of equation (1.24), as well as that of equation (1.17a), after N terms, where N is a relatively small integer such that $\lambda_N \xi$ may still be treated as a small quantity. That it is possible to find such an integer, without destroying the accuracy of the series in which the truncations are made, must be verified after the solutions are obtained.

We shall also restrict the solution to the case where ξ is large enough to make $e^{-\lambda_N \xi}$ negligible compared to one. The error incurred by doing this is less than ten per cent for ξ greater than 0.6, and less than five per cent for ξ greater than 0.8. Actually, it may be anticipated that this assumption does not restrict the value of ξ any more than it already is restricted by the assumption that η is small; this, too, can be checked after the solutions are

obtained. Nevertheless, with this assumption, both $\sinh \lambda_n \xi$ and $\cosh \lambda_n \xi$ may be represented very accurately by exponential functions, since

$$\left. \begin{array}{l} \sinh \lambda_n \xi \\ \cosh \lambda_n \xi \end{array} \right\} = \frac{1}{2} e^{\lambda_n \xi} \left[1 + O(\{e^{-\lambda_n \xi}\}^2) \right]$$

Thus, substituting the complete expression for ϕ into equation (1.9) and keeping first-order terms only, we find:

$$(IV) \quad \frac{\partial \mathcal{J}}{\partial \xi} = \frac{1}{2} \sum_{n=1}^N B_n \lambda_n e^{\lambda_n \xi} J_0(\lambda_n \eta) \quad (1.25)$$

in which we have also assumed that $\frac{\partial \mathcal{J}}{\partial \xi}$ is not less than order \mathcal{J} . (Again, this may be verified with the final solutions.) We note then that a series whose coefficients behave like $B_n e^{\lambda_n \xi}$ is of order \mathcal{J} or more. Finally, substituting the expression for ϕ into equation (1.10), we find:

$$(V) \quad \begin{aligned} & 4 \sum_{n=1}^N A_n \lambda_n e^{-\lambda_n \xi} J_0(\lambda_n \eta) + \sum_{n=1}^N (B_n' + \lambda_n B_n) e^{\lambda_n \xi} J_0(\lambda_n \eta) - \\ & - \frac{2}{8F^2} \frac{1}{\eta} \frac{\partial}{\partial \eta} \left(\eta \frac{\partial \mathcal{J}}{\partial \eta} \right) + \frac{2\mathcal{J}}{F^2} = 2 f_2(\xi) \end{aligned} \quad (1.26)$$

where primes denote differentiation with respect to ξ . Differentiating equation (1.26) with respect to ξ and using equation (1.25) to eliminate \mathcal{J} , there results:

$$\begin{aligned} & \sum_{n=1}^N \left\{ \left[B_n'' + 2 \lambda_n B_n' + \left(\frac{1}{F^2} + \lambda_n + \frac{\lambda_n^2}{8F^2} \right) \lambda_n B_n \right] e^{\lambda_n \xi} - \right. \\ & \left. - 4 A_n \lambda_n^2 e^{-\lambda_n \xi} \right\} J_0(\lambda_n \eta) = 2 f_2'(\xi) \end{aligned} \quad (1.27)$$

For a given value of ξ the right member of equation (1.27) is a constant, and hence the left member must be an expansion of that constant in a series of Bessel functions. However, since the set of functions $J_0(\lambda_n \eta)$, $n = 1, 2, 3, \dots$ ($0 \leq \eta \leq 1$), lacks a constant of being a complete set, both members of equation (1.27) must be zero, and, in fact, the left member must be zero term by term. We therefore have

$$\begin{aligned} B_n'' + 2\lambda_n B_n' + \left(\frac{1}{F^2} + \lambda_n + \frac{\lambda_n^2}{BF^2}\right) \lambda_n B_n &= \\ &= 4A_n \lambda_n^2 e^{-2\lambda_n \xi} \quad \text{for } n = 1, 2, \dots, N. \end{aligned} \quad (1.28)$$

Evaluating equations (1.25) and (1.26) when $\xi = \xi_0$ by using the initial conditions of equations (1.18) and (1.19), we find the following boundary conditions for B_n :

$$B_n(\xi_0) = 0 \quad (1.29)$$

$$B_n'(\xi_0) = -4A_n \lambda_n e^{-2\lambda_n \xi_0} \quad (1.30)$$

The solution for $B_n(\xi)$ is thus found to be:

$$\begin{aligned} B_n(\xi) = \frac{4A_n \lambda_n^2}{\omega_n^2 + \lambda_n^2} \left[e^{-\lambda_n(\xi_0 + \xi)} \left\{ \frac{\omega_n}{\lambda_n} \sin \omega_n(\xi_0 - \xi) - \right. \right. \\ \left. \left. - \cos \omega_n(\xi_0 - \xi) \right\} + e^{-2\lambda_n \xi} \right], \end{aligned} \quad (1.31a)$$

where

$$\omega_n = \frac{1}{F} \sqrt{\lambda_n \left(1 + \frac{\lambda_n^2}{B}\right)} \quad (1.31b)$$

Since equation (1.25) gives

$$\eta = \frac{1}{2} \sum_{n=1}^N \lambda_n J_0(\lambda_n \eta) \int_{\xi_0}^{\xi} B_n(\xi_1) e^{\lambda_n \xi_1} d\xi_1$$

we have

$$\begin{aligned} \eta = 2 \sum_{n=1}^N \frac{A_n \lambda_n^2 e^{-\lambda_n \xi_0}}{\omega_n^2 + \lambda_n^2} & \left[\cos \omega_n (\xi_0 - \xi) + \right. \\ & \left. + \frac{\lambda_n}{\omega_n} \sin \omega_n (\xi_0 - \xi) - e^{\lambda_n (\xi_0 - \xi)} \right] J_0(\lambda_n \eta) \end{aligned} \quad (1.32a)$$

If the Froude number F is either large or small compared to one, η has the following asymptotic forms:

$$\begin{aligned} \eta \approx 2 F^2 \sum_{n=1}^N \frac{A_n \lambda_n}{1 + \frac{\lambda_n^2}{B}} & \left[e^{-\lambda_n \xi_0} \cos \left\{ \frac{1}{F} \sqrt{\lambda_n \left(1 + \frac{\lambda_n^2}{B} \right)} (\xi_0 - \xi) \right\} - \right. \\ & \left. - e^{-\lambda_n \xi} \right] J_0(\lambda_n \eta) \quad \text{for } F \ll 1, \end{aligned} \quad (1.32b)$$

$$\begin{aligned} \eta \approx 2 \sum_{n=1}^N A_n & \left[e^{-\lambda_n \xi_0} \{ 1 + \lambda_n (\xi_0 - \xi) \} - e^{-\lambda_n \xi} \right] J_0(\lambda_n \eta) \\ \text{for } F \gg 1. \end{aligned} \quad (1.32c)$$

Thus, we see that the amplitude of the surface deformation is independent of F for large F , and proportional to F^2 for small F . Typical surface profiles indicated by equation (1.32c) are presented in Figures 2, 3, and 4, for $\delta = 0, .2$, and $.5$, respectively. The starting position ξ_0 has been taken to be infinite for these curves, but it is clear that the results are essentially independent of ξ_0 if ξ_0 is greater than 2, say. It should be noted that the profiles

shown in the figures indicate that, if δ is small, the deformations tend to grow quite rapidly when \mathfrak{F} reaches a value on the order of 0.7.

The solutions obtained for \mathfrak{F} have been based on the assumption that the series in equations (1.17a) and (1.24) are very rapidly convergent when \mathfrak{z} is of the order of \mathfrak{F} (only their behavior for values of \mathfrak{z} near the surface has been needed). It is now clear, using equation (1.31a), that for either series the ratio of any given term to the preceding term is roughly the order of $e^{-\pi \mathfrak{F}}$, since $\lambda_n - \lambda_{n-1} \approx \pi$. Since we are treating only the case in which \mathfrak{F} is large enough to make $e^{-\lambda_n \mathfrak{F}}$ negligible compared to one ($\lambda_1 = 3.832$), the truncation procedure is clearly justified.

It may now also be verified that for large F the assumption that $e^{-\lambda_n \mathfrak{F}}$ is negligible does not place any new restrictions on the acceptable range of \mathfrak{F} ; the curves in Figures 2, 3, and 4, for example, indicate that the linearization procedure will break down at about the same values of \mathfrak{F} as the above assumption.

Finally, it was assumed that $\frac{\partial \mathfrak{F}}{\partial \mathfrak{z}}$ is at least of order \mathfrak{F} ; equation (1.32a) indicates that this is indeed the case.

If the Froude number is not too large, equations (1.32a) and (1.32b) indicate that the shape of the surface is influenced by surface tension effects because of the formal dependence of \mathfrak{F} on the Bond number B . It should be noted, however, that, unless the radius a is so small that the cylinder becomes essentially a capillary tube, this Bond number dependence is extremely weak due to the large values of B . For example, if the radius of the cylinder is as small as ten

centimeters, and if the draining liquid is hydrazine (which has an unusually large coefficient of surface tension and, incidentally, is a common rocket propellant), then the Bond number is greater than 1000.

Although detailed experimental measurements of surface profiles have not been made (with which to compare the profiles in Figures 2, 3, and 4), it is possible to compare some of the general features of the flow predicted by equation (1.32a) with the experimental observations of Gluck, Gille, Zukoski, and Simkin⁴. They measured the height at which ingestion of the pressurization gas into the drain hole first occurs, i. e., at which $\mathcal{J}|_{\gamma=0} \equiv \mathcal{J}_0 = -\mathfrak{f}$. By plotting this "ingestion" height as a function of a Froude number Fr given by

$$Fr = \frac{F^2}{2\delta},$$

they found that the results appeared to be independent of δ .

Although the linearized analysis given here clearly does not apply to the case of the extreme surface deformation associated with actual gas ingestion, we may define a somewhat different critical position \mathfrak{f}_c at which $\mathcal{J}_0 = -\kappa \mathfrak{f}$, where κ is a constant small compared to one (rather than equal to one, as in the experiments). If Fr is not too small, the variation of \mathfrak{f}_c with Fr and δ should be similar to that of the measured ingestion height.

If we take N to be one, and \mathcal{J}_0 to be very large, equation (1.32a) predicts the following dependence of \mathfrak{f}_c on Fr and δ :

$$\mathfrak{f}_c e^{\lambda_1 \mathfrak{f}_c} = \left[\frac{4}{\kappa \{\mathcal{J}_0(\lambda_1)\}^2} \right] \left[\frac{\mathcal{J}_1(\lambda_1 \delta)}{(\lambda_1^2 \delta + \frac{\lambda_1}{2 Fr})} \right]. \quad (1.33)$$

Equation (1.33) indicates that ξ_c asymptotically approaches a limiting value for large F_r , and the values of F_r at which ξ_c first drops significantly below this limit are of the order of one. The same is true for the ingestion height measured by Gluck, et al.

The dependence of ξ_c on δ indicated by equation (1.33) is very weak, and in fact, at a given F_r , the range of ξ_c as δ varies between .1 and .3125 (the values used in the experiments) is considerably less than the scatter in the experimental data. Hence the variation of ξ_c with δ implied by equation (1.33) is consistent with the experimental difficulty in finding a systematic dependence on δ .

The solutions obtained by Saad and Oliver¹⁵ are based on the assumption that, if the velocity of the mean surface is constant, and if the surface deformation is small, then the nonlinear terms in the Bernoulli equation (i. e., those terms which involve the velocity components) can be entirely neglected. This assumption is only valid, however, for small Froude numbers, in which case all velocities are indeed small. The present analysis shows that in the general case the terms in question do make a contribution to the linearized equations and in fact significantly influence the final results. (Saad and Oliver also explicitly assume that

$$F \ll \frac{1}{\delta} \sqrt{1 + \frac{\lambda_n^2}{B}}$$

so the range of F is strongly limited even if the Bernoulli equation is properly linearized.) Their basic approach is to linearize with respect to the quantity $(\xi_0 - \xi)$, as well as with respect to δ .

Under these assumptions for F small and \mathfrak{F}_0 relatively small, they find surface oscillations.

The set of initial conditions which leads to these oscillations requires careful examination. In formulating the initial conditions, Saad and Oliver state that they are considering the case in which the liquid is initially at rest; the surface is thus assumed to be undeformed (if the Bond number is not too small), and all initial velocities are zero. It thus appears that the effects of the starting transient are to be included in their analysis. However, in solving the problem they treat only the case in which U is a constant. Since they refer to this as "step function flow," it is clear that they are considering the flow to be started from rest, but to be accelerated instantaneously to the velocity U at the initial instant. Although no justification is given, they are obviously assuming that since the starting transient is likely to be very rapid (this point will be verified in Section 1.8), it has little effect on the phenomena involved in the deformation of the surface. To justify this assumption it must be shown that a characteristic time associated with the starting transient is small compared with a characteristic time associated with the deformation of the surface. It will be shown in Section 1.7, however, that this is in fact not the case when \mathfrak{F}_0 is not large. In other words, it will be shown that $\frac{\partial \mathfrak{F}}{\partial t} = O\left(\frac{\partial \mathfrak{F}}{\partial t}\right)$ during the starting transient, if \mathfrak{F}_0 is not large.

Thus, by setting U equal to a constant at the outset, Saad and Oliver have in effect used the same initial conditions as those in the present treatment. The solutions obtained in both treatments there-

fore apply to the case in which the surface is initially traveling downward with speed U and is constrained to lie in a horizontal plane; when $\mathfrak{F} = \mathfrak{F}_0$, this constraint is removed and the surface is allowed to deform. Equation (1.32b) shows that the present analysis also predicts surface oscillations if F is small and \mathfrak{F} is not too large.

The physical mechanism involved in creating the oscillation appears to be the following. For a given position \mathfrak{F} there exists an "equilibrium" surface profile, which we may define as that shape which the surface would have at \mathfrak{F} if it were started (with constant speed U) from a position \mathfrak{F}_0 much greater than \mathfrak{F} . It is clear that if \mathfrak{F} is large, this equilibrium profile is essentially a horizontal plane. Thus, the initial conditions given by equations (1.18) and (1.19) are realistic if \mathfrak{F}_0 is not small.

On the other hand, if \mathfrak{F}_0 is small, the assumed starting profile is quite different from the equilibrium profile, and restoring forces will drive the surface towards the equilibrium state; that is, relative to the mean height, the liquid at the center of the tank accelerates downward and that at the outer circumference accelerates upward. It is reasonable to assume that the magnitude of these restoring forces is a function of the amount by which the actual surface is displaced from the equilibrium profile. Thus, in a sense, this process possesses a certain momentum; that is to say, when the equilibrium profile is reached, the liquid in the center will have accelerated to a significant downward velocity relative to the liquid near the outer wall. Therefore, the surface profile will "overshoot"

the equilibrium profile in much the same way as a mass, oscillating on a spring, overshoots its equilibrium position every half-cycle; thus, the oscillation of the surface will continue under the action of the hydrodynamically supplied restoring forces.

The important point is that the oscillations are the result of a set of initial conditions which require the surface to be moving with an undeformed surface at the initial instant. If the starting position given by ξ_0 is relatively low, it would be extremely difficult to reproduce these initial conditions in a laboratory setup. Therefore, it must be concluded that for the case of small ξ_0 the initial conditions are unrealistic, and the surface oscillations which are predicted as a result of these initial conditions are of little physical significance.

1.7 Initial Accelerations

In this section we shall attempt to find the initial acceleration distribution across the surface when the flow is started from rest. It will now be assumed that the net pressure head, rather than the mass flow rate, is held constant. We shall again linearize with respect to quantities of order J ; this in no way compromises the accuracy of the final results, however, since we need only consider the flow during an infinitesimal time interval starting at the initial instant, which we shall take to be $\tau = 0$.

The notation will be essentially the same as that used in the previous sections, with the following exceptions and additions.

C_n = unknown coefficient in expression for ϕ (see equation (1.33))

$$F = \frac{U_c}{\sqrt{a g}} \quad (U_c \text{ is defined below})$$

p_a^* = pressure above the free surface

p_o^* = pressure at the origin

$$p_h^* = p_a^* - p_o^*$$

$$R = [\alpha_o]_{\eta=0} / [\alpha_o]_{\eta=1} \quad (\alpha_o \text{ is defined below})$$

$$t = \frac{t^*}{a/U_c}$$

$$U_c = \sqrt{\frac{p_h^*}{\rho}}$$

$$V^* = \frac{dh}{dt^*}$$

$$V = V^*/U_c$$

$$\alpha = \frac{\partial}{\partial t} (\xi + \eta)$$

$$\alpha_o = \alpha \Big|_{t=0}$$

$$\phi = \frac{\Phi^*}{U_c a}$$

The equations in this section will be nondimensionalized using $U_c = \sqrt{p_h^*/\rho}$ as a characteristic velocity, since we are primarily interested in the case of large mass flow rates and thus large pressure heads.

From the analysis of the previous sections it is obvious that the potential function ϕ must be of the following form:

$$\begin{aligned} \phi = V g - V \sum_{n=1}^{\infty} A_n \frac{\cosh \lambda_n (z - \xi)}{\sinh \lambda_n \xi} J_0(\lambda_n \eta) + \\ + \sum_{n=1}^{\infty} C_n(t) \cosh \lambda_n z J_0(\lambda_n \eta) \end{aligned}$$

where the coefficients $C_n(t)$ are unknown functions of time which permit ϕ to satisfy the free surface boundary conditions (IV) and (V). In the present notation, condition (IV) becomes:

$$(IV) \quad V + \frac{\partial \eta}{\partial t} = \left. \frac{\partial \phi}{\partial z} \right|_{z=\eta+\zeta} - \left. \frac{\partial \phi}{\partial \eta} \right|_{z=\eta+\zeta} \frac{\partial \eta}{\partial \eta} \quad (1.34)$$

If we evaluate the Bernoulli constant in condition (V) at the origin, we find:

$$(V) \quad 1 + \frac{1}{2} \left[\left(\frac{\partial \phi}{\partial z} \right)^2 + \left(\frac{\partial \phi}{\partial \eta} \right)^2 \right]_{z=\eta+\zeta} + \frac{\eta+\zeta}{F} + \left[\frac{\partial \phi}{\partial t} \right]_{z=\eta+\zeta} = \\ = \frac{V^2}{2g^4} + \left[\frac{\partial \phi}{\partial t} \right]_{\substack{z=0 \\ \eta=0}} \quad (1.35)$$

Although our primary interest is finding the acceleration distribution at time $t = 0$, we now have formally enough information to generate first-order equations for the unknown functions $C_n(t)$, $V(t)$, and $\eta(\eta, t)$. The problem is well-posed with the following initial conditions:

$$\eta \Big|_{t=0} = 0, \quad (1.36)$$

$$\frac{\partial \eta}{\partial t} \Big|_{t=0} = 0, \quad (1.37)$$

$$V \Big|_{t=0} = 0. \quad (1.38)$$

In substituting the expression for ϕ into equations (1.34) and (1.35), we shall make use of the fact that during the time interval considered, V , as well as t and η , is an infinitesimal quantity. Thus, keeping lowest order terms only, we find:

$$(IV) \quad \frac{\partial \xi}{\partial t} = \sum_{n=1}^{\infty} C_n \lambda_n \sinh \lambda_n \xi J_0(\lambda_n \eta), \quad (1.39)$$

and

$$(V) \quad \sum_{n=1}^{\infty} \left\{ C_n' \cosh \lambda_n \xi - V' \frac{A_n}{\sinh \lambda_n \xi} \right\} J_0(\lambda_n \eta) = \\ = - \left(1 + \frac{\xi}{F^2} \right) - V' \left(\xi + \sum_{n=1}^{\infty} A_n \coth \lambda_n \xi \right) + \sum_{n=1}^{\infty} C_n', \quad (1.40)$$

where primes now denote differentiation with respect to ξ . We again note that since the set of Bessel functions in equation (1.40) lacks a constant of being a complete set, all the terms in the series must be zero. Thus we have:

$$C_n' = \frac{A_n V'}{\sinh \lambda_n \xi \cosh \lambda_n \xi}, \quad (1.41)$$

and

$$\sum_{n=1}^{\infty} C_n' = \left(1 + \frac{\xi}{F^2} \right) + V' \left(\xi + \sum_{n=1}^{\infty} A_n \coth \lambda_n \xi \right). \quad (1.42)$$

Combining equations (1.41) and (1.42) to eliminate C_n' , we find:

$$V' = - \frac{\left(1 + \frac{\xi}{F^2} \right)}{\xi + \sum_{n=1}^{\infty} A_n \tanh \lambda_n \xi}. \quad (1.43)$$

We note that the quantity $\left(1 + \frac{\xi}{F^2} \right)$ is the total head acting on the liquid in the tank; the pressure head has been normalized to one, and ξ / F^2 is the nondimensionalized gravitational head.

Finally, putting the expression for V' into equation (1.41), there results:

$$C_n' = - \frac{2 A_n \left(1 + \frac{f}{F^2}\right)}{(\sinh 2 \lambda_n f) \left(f + \sum_{m=1}^{\infty} A_m \tanh \lambda_m f\right)} \quad (1.44)$$

We seek the dimensionless acceleration α :

$$\alpha = \frac{\partial^2 f}{\partial t^2} (f + f) = V' + \frac{\partial^2 f}{\partial t^2}$$

The quantity $\frac{\partial^2 f}{\partial t^2}$ is obtained by differentiating equation (1.39):

$$\frac{\partial^2 f}{\partial t^2} = \sum_{n=1}^{\infty} \lambda_n \left\{ C_n' \sinh \lambda_n f + C_n \lambda_n V \cosh \lambda_n f \right\} J_0(\lambda_n r) \quad (1.45)$$

Because of equation (1.39), initial condition (1.37) implies that

$C_n(0) = 0$ for all n , and we have

$$\left. \frac{\partial^2 f}{\partial t^2} \right|_{t=0} = \sum_{n=1}^{\infty} \lambda_n C_n'(0) \sinh \lambda_n f_0 J_0(\lambda_n r), \quad (1.46)$$

or, substituting the expression for C_n' of equation (1.44),

$$\left. \frac{\partial^2 f}{\partial t^2} \right|_{t=0} = - \left(1 + \frac{f_0}{F^2}\right) \sum_{n=1}^{\infty} \frac{A_n \lambda_n J_0(\lambda_n r)}{(\cosh \lambda_n f_0) \left(f_0 + \sum_{m=1}^{\infty} A_m \tanh \lambda_m f_0\right)} \quad (1.47)$$

Thus,

$$\alpha_0 = - \frac{\left(1 + \frac{f_0}{F^2}\right)}{f_0 + \sum_{m=1}^{\infty} A_m \tanh \lambda_m f_0} \left[1 + \sum_{n=1}^{\infty} \frac{A_n \lambda_n J_0(\lambda_n r)}{\cosh \lambda_n f_0} \right] \quad (1.48)$$

A useful parameter which may be taken as a measure of the initial tendency of the surface to deform is the ratio R of the initial acceleration at the center to the initial acceleration at the outer wall:

$$R = \frac{\alpha_0 \Big|_{\eta=0}}{\alpha_0 \Big|_{\eta=1}} = \frac{1 + \sum_{n=1}^{\infty} \frac{A_n \lambda_n}{\cosh \lambda_n \xi_0}}{1 + \sum_{n=1}^{\infty} \frac{A_n \lambda_n}{\cosh \lambda_n \xi_0} J_0(\lambda_n)} \quad (1.49)$$

The dependence of R on ξ_0 and δ is indicated graphically in Figure 5. For ξ_0 greater than about 1.2 there is clearly very little tendency for the surface to deform. This indicates that the initial conditions assumed in Section 1.6 may be considered realistic for ξ_0 of that order or larger.

A curious property of equation (1.49) is that R is independent of the total head acting on the liquid. This means, for example, for a very low value of ξ_0 , the initial tendency of the surface to deform is extremely large, even if the total head on the liquid is quite small. This implies that the surface accelerates very rapidly (with respect to the displacement of the mean surface height) towards its "equilibrium" position, which it would have at ξ_0 if started from a greater initial height, even though that equilibrium position may represent only a very slight surface deformation.

We have seen that $C_n(0) = 0$, and thus, using equation (1.44), the Taylor series expansion for $C_n(t)$ about the point $t = 0$ must be of the form

$$C_n(t) = - \frac{2 A_n \left(1 + \frac{\xi_0}{F^2} \right) t}{(\cosh \lambda_n \xi_0) \left(\xi_0 + \sum_{m=1}^{\infty} A_m \tanh \lambda_m \xi_0 \right)} + O(t^2) \quad (1.50)$$

Similarly, using equations (1.43) and (1.38),

$$V(t) = - \frac{\left(1 + \frac{\xi_0}{F^2}\right) t}{\xi_0 + \sum_{n=1}^{\infty} A_n \tanh \lambda_n \xi_0} + O(t^2) . \quad (1.51)$$

Therefore,

$$\frac{C_n}{V} = \frac{2 A_n}{\sinh 2 \lambda_n \xi_0} + O(t) . \quad (1.52)$$

Using equation (1.39),

$$\frac{\partial \mathcal{F}}{\partial \xi} = \frac{1}{V} \frac{\partial \mathcal{F}}{\partial t} = \sum_{n=1}^{\infty} \frac{C_n}{V} \lambda_n \sinh \lambda_n \xi J_0(\lambda_n \eta) + O(t) \quad (1.53)$$

or

$$\left. \frac{\partial \mathcal{F}}{\partial \xi} \right|_{t=0} = \sum_{n=1}^{\infty} \frac{A_n \lambda_n}{\cosh \lambda_n \xi_0} J_0(\lambda_n \eta) , \quad (1.54)$$

Thus, we see that if ξ_0 is not too large, $\left. \frac{\partial \mathcal{F}}{\partial \xi} \right|_{t=0}$ is of order one, that is,

$$\frac{\partial \mathcal{F}}{\partial t} = O\left(\frac{\partial \mathcal{F}}{\partial t}\right) . \quad (1.55)$$

It follows that the "step-function flow" assumption of Saad and Oliver, that the starting transient precedes any significant surface deformations is clearly invalid. Equation (1.55) also shows, because of the large acceleration ratios indicated in Figure 5, that one may expect the starting transient itself to be very rapid, or, more precisely, to occur during a very small displacement of the mean surface position. This will be investigated in the next section.

It should be noted that the solutions for α_0 and R found in this section are exact solutions of the potential-flow problem as

formulated, regardless of the magnitude of α_0 or R . (Since the surface is initially undeformed, surface tension effects do not enter, regardless of the size of the surface tension coefficient, assuming the contact angle with the wall is zero.)

1.8 Zeroth-order Starting Transient

We now consider the zeroth-order variation of the mean height if the flow is started from rest and the pressure head is held constant. By definition, the zeroth-order flow is that which results when the surface is constrained to lie in a horizontal plane. We shall denote by the quantity U_0^* the quantity $\frac{dh}{dt^*}$, and by U_0 the parameter U_0^*/U_c . Otherwise, the notation will be essentially the same as in the previous section.

It may be anticipated that the first-order correction to U_0 is relatively small, except at low surface heights, for the following reason. The average pressure, integrated over the surface, is always p_a^* , and thus always equal to the value it would have if the surface were allowed to deform. In addition, the difference in the pressure distribution on the bottom of the tank for the zeroth- and first-order flows will be very small even when the first-order surface deformations are significant, as long as the height η is not too small. (Of course, the pressure near the origin is assumed to be the same in both cases.) Thus, the total force acting on the liquid and controlling the mass flow rate will be roughly the same for the two cases. (It will be possible to verify this hypothesis to a limited extent when the solution is obtained.)

The flow field for the zeroth-order starting transient is equivalent to the flow which results if on the surface of the liquid there is a weightless, frictionless piston, above which there is a pressure p_a^* . (This, of course, is not the same as having a piston of weight $p_a^* \pi a^2$ because of the dynamics of the piston.) The only initial condition that is required is

$$U_0 \Big|_{\xi=\xi_0} = 0, \quad (1.56)$$

and we again note that it will be convenient to use ξ instead of t as the independent variable. To this end, we observe $\frac{\partial}{\partial t} = U_0 \frac{\partial}{\partial \xi}$.

As we have seen, the potential function must be of the following form:

$$\phi_0 = U_0 \xi - U_0 \sum_{n=1}^{\infty} A_n \frac{\cosh \lambda_n (\xi - \xi_0)}{\sinh \lambda_n \xi} J_0(\lambda_n \eta). \quad (1.57)$$

We shall again use the Bernoulli integral to generate the governing dynamical equation. Evaluating the Bernoulli constant first at the surface and secondly in the exit hole, and then averaging, respectively, over the surface and over the plane of the exit hole, we find:

$$\begin{aligned} \left(1 + \frac{\xi^2}{F^2}\right) + \frac{U_0^2}{2} + \int_0^1 \left[\left(\frac{\partial \phi_0}{\partial \eta} \right)^2 \right]_{\xi=\xi} \eta d\eta + 2U_0 \int_0^1 \left[\frac{\partial \phi_0}{\partial \xi} \right]_{\xi=\xi} \eta d\eta = \\ = \frac{U_0^2}{2\delta^4} + \frac{1}{\delta^2} \int_0^{\delta} \left[\left(\frac{\partial \phi_0}{\partial \eta} \right)^2 \right]_{\xi=0} \eta d\eta + \frac{2U_0}{\delta^2} \int_0^{\delta} \left[\frac{\partial \phi_0}{\partial \xi} \right]_{\xi=0} \eta d\eta, \end{aligned} \quad (1.58)$$

in which we have assumed that p_a^* is now the average pressure in the plane of the hole, rather than simply the pressure at the origin.

When substituting the expression for ϕ_0 into this equation, we shall restrict the solutions to values of ξ not very small by assuming that $e^{-2\lambda_n \xi}$ is negligible compared to one. The error incurred is, for example, less than ten per cent if ξ is greater than 0.3, and less than one per cent if ξ is greater than 0.6. We shall also assume that δ^2 is negligible compared to one. Thus, we find:

$$\frac{dU_0^2}{d\xi} + \left[\frac{-1/\delta^4}{\xi + \frac{2}{\delta} \sum_{n=1}^{\infty} \frac{A_n}{\lambda_n} J_1(\lambda_n \delta)} \right] U_0^2 = \frac{-2 \left(1 + \frac{\xi}{F^2} \right)}{\xi + \frac{2}{\delta} \sum_{n=1}^{\infty} \frac{A_n}{\lambda_n} J_1(\lambda_n \delta)}, \quad (1.59)$$

which is subject to the initial condition $U_0^2 \Big|_{\xi=\xi_0} = 0$. After some algebraic manipulation the solution for U_0^2 may be written as follows.

$$U_0^2 = \left[\delta^4 \left(\lambda - \frac{4}{F^2 \delta} \sum_{n=1}^{\infty} \frac{A_n}{\lambda_n} J_1(\lambda_n \delta) \right) \right] \left[1 - \left(\frac{1 + \frac{\delta \xi}{2 \sum_{n=1}^{\infty} \frac{A_n}{\lambda_n} J_1(\lambda_n \delta)}}{1 + \frac{\delta \xi_0}{2 \sum_{n=1}^{\infty} \frac{A_n}{\lambda_n} J_1(\lambda_n \delta)}} \right)^{1/\delta^4} \right] + \left[\frac{2\delta^4}{F^2} \left(\xi + \frac{2}{\delta} \sum_{n=1}^{\infty} \frac{A_n}{\lambda_n} J_1(\lambda_n \delta) \right) \right] \left[1 - \left(\frac{1 + \frac{\delta \xi}{2 \sum_{n=1}^{\infty} \frac{A_n}{\lambda_n} J_1(\lambda_n \delta)}}{1 + \frac{\delta \xi_0}{2 \sum_{n=1}^{\infty} \frac{A_n}{\lambda_n} J_1(\lambda_n \delta)}} \right)^{\frac{1}{\delta^4} - 1} \right]. \quad (1.60)$$

In the final bracket in this expression, the exponent $(\frac{1}{\delta^4} - 1)$ may accurately be replaced by $1/\delta^4$ even if the factor on which the exponent appears is significantly less than one, since in that event the factor raised to either power is an extremely small number, which is to be subtracted from one. Thus, there finally results:

$$U_o = - \left\{ \left[1 - \left(\frac{1 + \frac{\delta \mathcal{F}}{2 \sum_{n=1}^{\infty} \frac{A_n}{\lambda_n} J_1(\lambda_n \delta)}}{1 + \frac{\delta \mathcal{F}_o}{2 \sum_{n=1}^{\infty} \frac{A_n}{\lambda_n} J_1(\lambda_n \delta)}} \right)^{1/4} \right] \left[2 \delta^4 \left(1 + \frac{\mathcal{F}}{F^2} \right) \right] \right\}^{1/2} \quad (1.61)$$

Of course, the functional dependence of \mathcal{F} on t is formally implied by the relation

$$\int_{\mathcal{F}_o}^{\mathcal{F}} \frac{d\mathcal{F}_1}{U_o(\mathcal{F}_1)} = t \quad (1.62)$$

Equation (1.61), however, is in a particularly useful form.

The quantity in the second set of rectangular brackets is exactly the "quasi-steady" result obtained for a slowly draining tank. The other set of rectangular brackets gives precisely the transient effects. Although its initial value is zero, it goes very rapidly to one because the exponent is an extremely large number. Hence, the starting transient occurs over an extremely small distance, regardless of the size of the total head $(1 + \frac{\mathcal{F}}{F^2})$, as anticipated in the previous section.

A partial check on the accuracy of the zeroth-order analysis can be made by comparing the initial acceleration which it predicts with the exact value obtained in Section 1.7. We note that

$$\left. \frac{dU_o}{dt} \right|_{t=0} = \frac{1}{2} \left. \frac{dU_o^2}{d\mathcal{F}} \right|_{\mathcal{F}=\mathcal{F}_o} \quad (1.63)$$

Using equation (1.59) we have

$$\left. \frac{dU_o}{dt} \right|_{t=0} = - \frac{(1 + \frac{\mathcal{F}_o}{F^2})}{\mathcal{F}_o + \frac{2}{\delta} \sum_{n=1}^{\infty} \frac{A_n}{\lambda_n} J_1(\lambda_n \delta)} \quad (2.64)$$

Equation (1.43) gives the exact result as

$$\left. \frac{dV}{dt} \right|_{t=0} = - \frac{(1 + \frac{\xi_0}{F^2})}{\xi_0 + \sum_{n=1}^{\infty} A_n \tanh \lambda_n \xi_0} \quad (1.65)$$

Equation (1.65), however, is based on the assumption that p_o^* is defined as the pressure at the origin, while equation (1.64) is based on the assumption that p_o^* is the average pressure across the plane of the exit hole. Hence these two results are comparable only in the limit of very small δ . However, the data in Figures 2 through 5 show that surface deformations are largest as δ tends to zero, and thus this case is the severest test of the accuracy of the zeroth-order analysis.

Therefore, defining Γ to be the ratio of the zeroth-order result to the exact result, we have, in the limit of small δ ,

$$\lim_{\delta \rightarrow 0} \Gamma = \frac{\xi_0 + \sum_{n=1}^{\infty} \frac{\tanh \lambda_n \xi_0}{\lambda_n [J_0(\lambda_n)]^2}}{\xi_0 + \sum_{n=1}^{\infty} \frac{1}{\lambda_n [J_0(\lambda_n)]^2}} \quad (1.66)$$

since

$$\lim_{\delta \rightarrow 0} A_n = \frac{1}{\lambda_n [J_0(\lambda_n)]^2} \quad (1.67)$$

If ξ_0 is greater than 0.5, the two series in equation (1.66) differ by less than five per cent, and thus Γ differs from one by even less. Thus we see that if δ^2 is very small and ξ is greater than about 0.5, the transient behavior is well represented by equation (1.61).

1.9 Concluding Remarks

The solution for the deformation of the surface given by equation (1.32a) is valid (unlike previously available solutions) for the

physically important case of large F and large values of $(\xi_0 - \xi)$. It is the surface profiles which correspond to this case which are given in Figures 2, 3, and 4.

We have seen that $\left. \frac{\partial \xi}{\partial t} \right|_{t=0}$, given by equation (1.54), as well as the transient behavior of the mean surface when accelerated from rest, as given by the first set of rectangular brackets in equation (1.61), is independent of the total head on the fluid in the tank. It should be noted, of course, that this does not mean that the accelerations which occur during the starting transient are independent of the total head, but rather that the distances over which the transient effects take place are themselves independent of the total head. Thus, if ξ_s is defined as the value of ξ at which the starting transient is essentially completed (ξ_s may be defined, for example, as the value of ξ for which $|U_s|$ is a maximum), then $\xi_0 - \xi_s$ is virtually independent of the total head, but the time required for ξ to reach ξ_s clearly decreases as the total head increases. An important result of Sections 1.7 and 1.8 is that ξ_s will be very close to ξ_0 , but that the amplitude of the surface deformation when $\xi = \xi_s$ will be significant if ξ_0 is not large. Thus, any attempt to find the surface profiles when the flow is started from rest must properly take into account the surface deformation which occurs during the starting transient.

As noted earlier, the primary application of the problem considered is in the design of rocket propellant tanks. Since the surface deformation can lead to the ingestion of pressurization gas into the

propellant lines while a significant amount of propellant remains in the tank, it becomes a propellant utilization problem. The emphasis here has been on calculating the surface deformations which occur for the tank geometry indicated in Figure 1. A related problem, which could prove to be an area of fruitful research in the future, would involve trying to optimize the tank geometry to minimize the amount of unused propellant remaining when gas ingestion occurs. A conical geometry, for example, might lend itself to a theoretical analysis, and the opportunities for experimental investigations are virtually unlimited.

PART II. STABILITY OF A LAMINAR FILM
ON AN INCLINED PLANE

2. 1. Introduction

In this part we shall investigate the stability characteristics of a laminar film on an inclined plane. Because of the presence of the free surface, this problem is in many respects quite different from the classical problems in hydrodynamic stability. Many of these differences become readily apparent when a comparison is made with the problem of the stability of plane Poiseuille flow between parallel walls. The Poiseuille flow is roughly the equivalent of the laminar film with the free surface eliminated; if one regards the plane of the undisturbed free surface of the film as corresponding to the plane of symmetry in the Poiseuille flow, the undisturbed velocity distributions in the two flow fields will be identical.

The stability of plane Poiseuille flow has been extensively treated in the literature, notably by Lin¹³, Heisenberg⁶, and Shen¹⁶. The flow is found to be stable for values of the Reynolds number (based on the mean flow velocity and the channel half-width) less than about 4000, at which point the transition to turbulence begins. On the other hand, for the laminar film, the transition to turbulence is known to occur at Reynolds numbers on the order of 300. (See, for example, Jeffreys⁷.) Thus, the free surface is seen to have a destabilizing effect.

It has, however, a much more profound effect than that; it introduces, in effect, an additional degree of freedom, and this leads to a different mode of instability which is observed throughout almost the entire laminar flow regime. Instead of parallel laminar flow with straight streamlines, there is observed a wavy laminar flow with

visible surface waves propagating in the direction of flow, even at Reynolds numbers as low as ten or less. It is the stability with respect to the transition to this wavy flow regime that is treated here.

The problem has long been of interest to chemical engineers concerned with the properties of films of condensing vapors. A number of attempts have been made to measure experimentally the so-called critical Reynolds number, defined as that Reynolds number below which infinitesimal disturbances are positively damped, making the parallel laminar flow stable, and above which at least some kinds of infinitesimal disturbances are negatively damped, leading to waves of finite amplitude. Friedman and Miller³ studied the flow of thin films down the outside of a vertical cylinder, and noted an apparent critical Reynolds number on the order of six. Grimley⁵, using both cylinders and plane surfaces, determined the critical value to be 6.2. On the other hand, Binnie², using an optical system capable of detecting waves of very small amplitude, obtained photographs of unmistakable wave trains at Reynolds numbers as low as 4.4.

Perhaps the most sensitive experimental setup for detecting the waves, however, was designed, somewhat unwittingly, by Kirkbride⁹ in 1934 for an experiment designed to measure heat transfer coefficients. In first trying to correlate the friction factor with Reynolds number, he observed a systematic deviation from the accepted theoretical curve for Reynolds numbers greater than about two. Since his measured values for the film thickness were apparently too large, and since his experimental setup (involving a micrometer device which was moved until contact could just be maintained between

the liquid and the micrometer) actually measured maximum film thickness rather than average film thickness, he was forced to conclude that waves, which could not be observed visually, were in fact present. He therefore, in effect, measured a critical Reynolds number of about two. Thus, although there is a considerable spread in the experimental results, there is also an obvious trend; as techniques for detecting the presence of waves become more sensitive, the measured value of the critical Reynolds number decreases.

From the theoretical point of view, the desired end result, of course, is not merely a value for the critical Reynolds number, but, as in other problems in hydrodynamic stability, a curve of neutral stability in the R - α plane (R is the Reynolds number, and α , the nondimensional wave number). Each point on such a curve indicates the wave number (or wavelength) of an infinitesimal sinusoidal disturbance which, at the corresponding Reynolds number, is undamped. Such a curve in general separates a region of stability (positive damping) and a region of instability (negative damping), and the minimum value of R along such a curve corresponds to the critical Reynolds number. In the classical problems, as well as in the present problem, the primary difficulty in finding a neutral-stability curve is solving the Orr-Sommerfeld equation, which the first-order stream-function must satisfy. The approach almost always used, with considerable success, is based on the assumption that the reciprocal of the Reynolds number is a small quantity; this clearly is not the case in the current problem, and an alternate approach is required.

On the other hand, a significant difficulty common to most of

the classical stability problems is averted in this case by the presence of the free surface. In the usual case, the speed of propagation of the disturbance is not large enough to exceed the zeroth-order (undisturbed) flow speed at all points in the flow. Thus there exists a layer in the flow that travels with the same speed as the wave disturbance, and hence fluid particles in that layer remain at a constant phase of the wave motion. This is the primary mechanism for the energy input into the first-order flow, and is reflected by serious difficulties in the mathematical formulation of the problem.

That these difficulties are not likely to occur in the present problem can be seen in the following way. For the case of long waves, the theory of kinematic waves developed by Lighthill and Whitham^{1 2} is applicable. They showed that when the volume flow rate past a given point is a function only of "concentration" (in this case, film thickness), continuity considerations alone are sufficient to determine the speed of propagation of long wavelength disturbances. For the parabolic velocity distribution of the zeroth-order flow of the present problem, this leads to a prediction of a wave speed exactly twice as large as the maximum flow speed. Thus, in sharp contrast to the case of plane Poiseuille flow, for which there is no analog to the kinematic wave, the indicated difficulties should not arise for small wave numbers. (This therefore appears to be one of the rare cases in which mathematical difficulties are eliminated, rather than created, by the introduction of a free surface.)

The problem has been attacked theoretically only relatively recently, and in each case, the approach has been to obtain approxi-

mate solutions to the Orr-Sommerfeld equation by assuming that the product of the wave number and the Reynolds number is a small quantity. Only two quantitative estimates of the neutral stability curves have been given, the first by Yih¹⁹ in 1954 for the case of a film with no surface tension on a vertical wall, and the second by Benjamin¹ in 1957 for the more general case of arbitrary surface tension coefficient and arbitrary wall inclination. Benjamin's results appeared to contradict those of Yih, and in 1963 Yih²⁰ conceded that the numerical calculations on which his solutions were based were "not accurate enough." Using an approach similar to that used in 1954 he was able to show, without obtaining quantitative results, that the general features of Benjamin's neutral stability curves appeared to be correct.

Although Benjamin's curves were accurate only in a small neighborhood of the R -axis, their significance lay in the fact that they implied, for a vertical wall, a critical Reynolds number of zero, i. e., that the film was unstable at all Reynolds numbers. They also indicated, for the first time, that the shapes of the neutral-stability curves were quite different from the distinctive shapes associated with the classical hydrodynamic stability problems. (A more detailed account of the theoretical work in this problem is given in Section 2.4.)

A new approach is suggested in Section 2.5 for obtaining approximate solutions to the Orr-Sommerfeld equation. The resulting solutions for the neutral-stability curves are valid over a much larger domain in the R - α plane than those previously obtained. In the case of small α , however, they provide the first quantitative confirmation of Benjamin's surprising results.

In the literature, there has also been considerable confusion regarding the existence of undamped waves for the case (originally studied by Yih) of a film with zero surface tension on a vertical wall. Benjamin¹ has tentatively suggested that undamped waves do exist, i. e., that there is a neutral stability curve in the first quadrant of the R - α plane, but Yih²⁰ concluded in 1963 that the entire first quadrant is a region of instability. In 1965, however, Yih²¹ corrected algebraic errors in his 1963 paper and apparently proved that undamped waves do indeed exist. In Section 2.7, a proof is given that undamped waves of the type considered by Yih cannot in fact exist, and a possible source of error in Yih's proof to the contrary is suggested.

2.2. Notation

The following notation will be used throughout Part II.

Dimensional parameters (see Figure 6):

- c^* = wave speed of disturbance wave motion
- E_{ij} = elements of the stress tensor
- g = acceleration due to gravity
- h^* = local film thickness
- h_o^* = film thickness of undisturbed flow
- p^* = pressure
- t^* = time
- \bar{T} = stress acting on the film surface
- \bar{T}_x, \bar{T}_y = components of \bar{T}
- $U_c = \frac{g h_o^{*2}}{3\nu} \sin \omega$ = mean speed of undisturbed flow
- u^* = x-component of velocity

v^* = y-component of velocity

x^* = coordinate measuring distance along the wall

y^* = coordinate measuring normal distance from the wall

λ = wavelength of disturbance wave motion

ν = coefficient of viscosity

$\nu = \frac{\mu}{\rho}$ = kinematic coefficient of viscosity

ρ = density

σ = coefficient of surface tension

Dimensionless parameters:

A_1, A_2, B_1, B_2 = constants of integration (see equation (2.51))

$c = \frac{c^*}{U_c}$

$h = \frac{h^*}{h_0^*}$

$i = \sqrt{-1}$

K_1, K_2, K_3, K_4 = functions defined by equations (2.56), (2.57), (2.58), and (2.59)

\hat{n} = unit normal vector at the surface

n_x, n_y = components of \hat{n} .

$p = \frac{p^*}{\rho U_c^2}$

P_0 = zeroth-order part of p

P_1 = first-order part of p which does not vary with the phase of the wave

p_1 = first-order part of p which travels with the wave disturbance

q = a function defined by equation (2.54)

$R = \frac{U_c h_0^*}{\nu}$ = Reynolds' number

S = a function defined by equation (2.60)

$$t = \frac{t^*}{h_o^*/u_c}$$

\hat{t} = unit tangent vector at the surface

t_x, t_y = components of \hat{t}

$$u = \frac{u^*}{U_c}$$

U_o = zeroth-order part of u

U_1 = first-order part of u which does not vary with the phase of the wave

u_1 = first-order part of u which travels with the wave disturbance

$$v = \frac{v^*}{U_c}$$

v_1 = first-order part of v

$$\kappa = \frac{\kappa^*}{h_o^*}$$

$$\eta = \frac{\eta^*}{h_o^*}$$

$$\alpha = \frac{2\pi h_o^*}{\lambda} = \text{nondimensionalized wave number}$$

β_1 = first-order correction to mean flow thickness

$$\delta = \frac{\sigma}{\rho} \left(\frac{3}{\nu^4 g} \right)^{1/3}$$

η_1 = first-order correction to film thickness due to wave motion $\left(\beta_1 + \eta_1 = \frac{h^* - h_o^*}{h_o^*} \right)$

θ_1 = amplitude of oscillations given by η_1

ϵ = per cent error in approximation involving $(c - U_o)$

$\bar{\epsilon}$ = average value of ϵ

λ_1, λ_2 = functions defined by equations (2.52) and (2.53)

ϕ_1 = y-dependent part of first-order streamfunction

ψ_1 = first-order streamfunction

ω = angle of inclination of the wall with respect to the horizontal

2.3. Formulation

The flow field whose stability we wish to investigate is the parallel laminar flow of a film of viscous liquid with a free surface, moving down a plane inclined at an angle ω with respect to the horizontal (see Figure 6). The flow is assumed to be at "terminal" conditions, i. e., the flow has established itself with an equilibrium velocity profile and constant film thickness, both of which are uniquely determined as a function of the mass flow rate, the angle ω , and the properties (viscosity and density) of the liquid.

For stability considerations, a two-dimensional analysis is of little value unless it can be proved that two-dimensional disturbances are indeed the first to become unstable. There does exist, however, a classic proof for the general hydrodynamic stability problem, first given by Squire¹⁷ in 1933, that two-dimensional disturbances have a greater tendency toward instability than three-dimensional disturbances. Squire showed that the mathematical formulation for the three-dimensional problem is identical to that for a two-dimensional problem at a lower Reynolds number, and hence the stability boundary is governed by two-dimensional effects.

The governing equations are the continuity equation and the Navier-Stokes equations of motion. In dimensionless notation, these become, respectively,

$$\frac{\partial u}{\partial x} + \frac{\partial v}{\partial y} = 0, \quad (2.1)$$

$$\frac{\partial u}{\partial t} + u \frac{\partial u}{\partial x} + v \frac{\partial u}{\partial y} = - \frac{\partial p}{\partial x} + \frac{1}{R} \left(\frac{\partial^2 u}{\partial x^2} + \frac{\partial^2 u}{\partial y^2} \right) + \frac{3}{R} \quad , \quad (2.2)$$

$$\frac{\partial v}{\partial t} + u \frac{\partial v}{\partial x} + v \frac{\partial v}{\partial y} = - \frac{\partial p}{\partial y} + \frac{1}{R} \left(\frac{\partial^2 v}{\partial x^2} + \frac{\partial^2 v}{\partial y^2} \right) - \frac{3}{R} \cot \omega \quad , \quad (2.3)$$

in which we have made use of the fact that $\frac{g h_0^*}{U_c^2} = \frac{3}{R \sin \omega}$

In solving the problem, we shall need the following boundary conditions.

(I) The shear stress at the surface must be continuous and thus zero (assuming the viscosity of the atmosphere is negligible compared to the viscosity of the liquid). The elements of the stress tensor are the following:

$$E_{xx} = -p^* + 2\mu \frac{\partial u^*}{\partial x^*} \quad ,$$

$$E_{yy} = -p^* + 2\mu \frac{\partial v^*}{\partial y^*} \quad ,$$

$$E_{xy} = \mu \left(\frac{\partial u^*}{\partial y^*} + \frac{\partial v^*}{\partial x^*} \right) \quad ,$$

and the unit normal vector \hat{n} (outward pointing) on the surface is defined by the following relations;

$$n_x = - \frac{\frac{\partial h}{\partial x}}{\left[1 + \left(\frac{\partial h}{\partial x} \right)^2 \right]^{1/2}} \quad ,$$

$$n_y = \frac{1}{\left[1 + \left(\frac{\partial h}{\partial x}\right)^2\right]^{1/2}} .$$

With these definitions, the stress \vec{T} acting on the surface is given by

$$T_x = E_{xx} n_x + E_{xy} n_y , \quad (2.4)$$

$$T_y = E_{xy} n_x + E_{yy} n_y . \quad (2.5)$$

The unit tangent vector \hat{t} is defined by the following relations:

$$t_x = n_y ,$$

$$t_y = -n_x .$$

Thus, the boundary condition becomes

$$(I) \quad \vec{T} \cdot \hat{t} = 0 ,$$

or

$$(I) \quad 2 \frac{\partial h}{\partial x} \left(\frac{\partial \sigma}{\partial y} - \frac{\partial \mu}{\partial x} \right) + \left(\frac{\partial \mu}{\partial y} + \frac{\partial \sigma}{\partial x} \right) \left(1 - \left[\frac{\partial h}{\partial x} \right]^2 \right) = 0 \quad \text{for } y = h . \quad (2.6)$$

(II) The normal stress must be continuous (and thus equal to the atmospheric pressure) at the free surface, except for a discontinuity arising from surface tension effects. Taking the atmospheric pressure to be zero, we must have

$$\vec{T} \cdot \hat{n} = \frac{\sigma \left(\frac{\partial^2 h}{\partial x^2} \right)}{\left[1 + \left(\frac{\partial h}{\partial x} \right)^2 \right]^{3/2}} .$$

Thus,

$$\begin{aligned}
 \text{(II)} \quad \left(\frac{\partial h}{\partial x}\right)^2 \left(-p + \frac{2}{R} \frac{\partial u}{\partial x}\right) - \frac{2}{R} \left(\frac{\partial u}{\partial y} + \frac{\partial v}{\partial x}\right) \left(\frac{\partial h}{\partial x}\right) + \\
 + \left(-p + \frac{2}{R} \frac{\partial v}{\partial y}\right) = \frac{\delta}{R^{4/3} (\sin \omega)^{1/3}} \frac{\frac{\partial^2 h}{\partial x^2}}{\left[1 + \left(\frac{\partial h}{\partial x}\right)^2\right]^{1/2}} \quad \text{for } y = h, \quad (2.7)
 \end{aligned}$$

in which $\delta = \frac{\sigma}{\rho} \left(\frac{3}{2\nu^2 g}\right)^{1/3}$.

(III) The no-slip condition at the wall requires

$$\text{(III)} \quad u = 0 \quad \text{for } y = 0. \quad (2.8)$$

(IV) Since there can be no normal velocity at the wall, we have

$$\text{(IV)} \quad v = 0 \quad \text{for } y = 0. \quad (2.9)$$

(V) Finally, we need the kinematical constraint that fluid particles in the surface remain in the surface:

$$\text{(V)} \quad \frac{\partial h}{\partial t} = v - u \frac{\partial h}{\partial x} \quad \text{for } y = h. \quad (2.10)$$

In order to linearize the equations, we expand the velocity components, the pressure, and the film thickness in the following manner.

$$\left. \begin{aligned}
 u &= u_0(y) + [u_1(y) + u_1(x, y, t)] + \dots \\
 v &= v_1(x, y, t) + \dots \\
 p &= p_0(y) + [p_1(y) + p_1(x, y, t)] + \dots \\
 h &= 1 + [\beta_1 + \eta_1(x, t)] + \dots
 \end{aligned} \right\} \quad (2.11)$$

The zeroth-order flow parameters associated with the undisturbed flow are indicated with the subscript \circ , while the subscript 1 denotes the first-order perturbation quantities associated with an infinitesimal wave disturbance.

The zeroth-order parts of the Navier-Stokes equations, equations (2.2) and (2.3), are

$$U_{\circ}'' + 3 = 0 \quad , \quad (2.12)$$

$$P_{\circ}' + \frac{3}{R} \cot \omega = 0 \quad , \quad (2.13)$$

where primes denote differentiation with respect to y . Only the first three boundary conditions have zeroth-order parts. These are

$$(I) \quad U_{\circ}'(1) = 0 \quad , \quad (2.14)$$

$$(II) \quad P_{\circ}(1) = 0 \quad , \quad (2.15)$$

$$(III) \quad U_{\circ}(0) = 0 \quad . \quad (2.16)$$

Thus we have the following solutions for $U_{\circ}(y)$ and $P_{\circ}(y)$:

$$U_{\circ}(y) = 3y \left(1 - \frac{y}{2}\right) \quad , \quad (2.17)$$

$$P_{\circ}(y) = \frac{3(1-y)}{R} \cot \omega \quad . \quad (2.18)$$

These relations determine the undisturbed flow and are exact solutions of the Navier-Stokes equations.

The lowest-order part of the continuity relation of equation (2.1) is

$$\frac{\partial u_1}{\partial x} + \frac{\partial v_1}{\partial y} = 0. \quad (2.19)$$

We therefore define a streamfunction ψ_1 such that

$$u_1 = \frac{\partial \psi_1}{\partial y}, \quad v_1 = -\frac{\partial \psi_1}{\partial x}.$$

Our goal is to find curves of neutral stability in the $R-\alpha$ plane; that is, for a given Reynolds number we wish to be able to find the wavelength of the infinitesimal sinusoidal wave (which may be regarded as a Fourier component of a general periodic wave) which has zero damping. We may therefore restrict our attention to the situation for which the wave profile has the form

$$\eta_1 = \Theta_1 e^{i\alpha(x - ct)} \quad (2.20)$$

and we shall look for solutions for the streamfunction ψ_1 of the following form:

$$\psi_1(x, y, t) = \phi_1(y) e^{i\alpha(x - ct)} \quad (2.21)$$

We note that undamped waves will occur when the imaginary part of c is equal to zero.

The first-order parts of the equations of motion are:

$$\frac{\partial u_1}{\partial t} + U_0 \frac{\partial u_1}{\partial x} + U_0' v_1 = -\frac{\partial p_1}{\partial x} + \frac{1}{R} \left(\frac{\partial^2 u_1}{\partial x^2} + U_1'' + \frac{\partial^2 u_1}{\partial y^2} \right), \quad (2.22)$$

$$\frac{\partial v_1}{\partial t} + U_0 \frac{\partial v_1}{\partial x} = -p_1' - \frac{\partial p_1}{\partial y} + \frac{1}{R} \left(\frac{\partial^2 v_1}{\partial x^2} + \frac{\partial^2 v_1}{\partial y^2} \right). \quad (2.23)$$

The first-order parts of the boundary conditions are:

$$(I) \quad -3(\beta_1 + \eta_1) + v_1'(1) + \frac{\partial u_1}{\partial y} + \frac{\partial w_1}{\partial x} = 0 \quad \text{for } y = 1, \quad (2.24)$$

$$(II) \quad \frac{3}{R} \cot \omega (\beta_1 + \eta_1) - p_1(1) - p_1 + \frac{2}{R} \frac{\partial w_1}{\partial y} = \frac{8 \left(\frac{\partial \eta_1}{\partial x} \right)}{R^{5/3} (\sin \omega)^{1/3}} \quad \text{for } y = 1, \quad (2.25)$$

$$(III) \quad v_1(0) + u_1 = 0 \quad \text{for } y = 0, \quad (2.26)$$

$$(IV) \quad w_1 = 0 \quad \text{for } y = 0, \quad (2.27)$$

$$(V) \quad \frac{\partial \eta_1}{\partial t} = w_1 - v_1 \frac{\partial \eta_1}{\partial x}. \quad (2.28)$$

Averaging equations (2.22) through (2.26) with respect to x over a wavelength, we find, respectively:

$$v_1''(y) = 0, \quad (2.29)$$

$$p_1'(y) = 0, \quad (2.30)$$

$$(I) \quad -3\beta_1 + v_1'(1) = 0, \quad (2.31)$$

$$(II) \quad \frac{3\beta_1}{R} \cot \omega - p_1(1) = 0, \quad (2.32)$$

$$(III) \quad v_1(0) = 0. \quad (2.33)$$

Thus we have:

$$v_1(y) = 3\beta_1 y, \quad (2.34)$$

$$P_1(y) = \frac{3\beta_1}{R} \cot \omega \quad (2.35)$$

We shall require, however, that the average mass flow rate of the perturbed flow past some station (say, $x = 0$) is the same as for the undisturbed flow:

$$\int_0^1 v_0 dy = \frac{\alpha c}{2\pi} \int_0^{\frac{2\pi}{\alpha c}} \left[\int_0^1 \left\{ v_0 + (v_1 + u_1) + \dots \right\} dy \right] dt \quad (2.36)$$

In performing the integration, we note that equation (2.28) implies

$$(V) \quad \phi_1(x) = (c - \frac{3}{2}) \phi_0 \quad (2.37)$$

Thus we find, from the first-order part of equation (2.36),

$$\beta_1 = 0 \quad (2.38)$$

Therefore,

$$v_1(y) = 0 \quad (2.39)$$

$$P_1(y) = 0 \quad (2.40)$$

Thus the average values of the film thickness, velocity profile, and pressure distribution, are unchanged by the wave motion.

Assuming the streamfunction is of the form given in equation (2.21), we can integrate equation (2.22) to obtain an expression for the first-order pressure variation p_1 :

$$p_1 = \left\{ \frac{1}{i\alpha R} (\phi_1''' - \alpha^2 \phi_1') + (c - v_0) \phi_1' + v_0' \phi_1 \right\} e^{i\alpha(x - ct)} \quad (2.41)$$

Then, by differentiating equation (2.22) with respect to y and equa-

tion (2.23) with respect to α and subtracting to eliminate the pressure, we obtain the differential equation which governs ϕ_1 , the well-known Orr-Sommerfeld equation:

$$-(c-u_0)(\phi_1'' - \alpha^2 \phi_1) - u_0'' \phi_1 = \frac{1}{i\alpha R} (\phi_1^{(iv)} - 2\alpha^2 \phi_1'' + \alpha^4 \phi_1) \quad (2.42)$$

It is now clear that all five boundary conditions are necessary; in addition to the four constants of integration in the general solution to equation (2.42), the free surface gives us an additional unknown parameter Θ_1 . (We have specified that the wave be sinusoidal and have wave number α ; only the amplitude, which is taken to be infinitesimal, is unknown.) In terms of ϕ_1 the boundary conditions become:

$$(I) \quad \phi_1''(1) + [\alpha^2(c - \frac{3}{2}) - 3] \Theta_1 = 0, \quad (2.43)$$

$$(II) \quad \phi_1'''(1) + \alpha \left[iR(c - \frac{3}{2}) - 3\alpha \right] \phi_1'(1) - i\alpha \left[\frac{\alpha^2 \delta}{R^{2/3} (\sin \omega)^{1/3}} + 3\omega \right] \Theta_1 = 0, \quad (2.44)$$

$$(III) \quad \phi_1'(0) = 0, \quad (2.45)$$

$$(IV) \quad \phi_1(0) = 0, \quad (2.46)$$

$$(V) \quad \phi_1(1) - (c - \frac{3}{2}) \Theta_1 = 0. \quad (2.47)$$

We see that if one finds four linearly independent solutions of the Orr-Sommerfeld equation, boundary conditions (I) through (V) become linear homogeneous equations for the four constants of integration and Θ_1 . A nontrivial solution will therefore exist only if the determinant of the coefficients vanishes. Setting the determinant equal to zero yields a complex equation involving α , R , c , ω , and δ .

Thus, we have generated an eigenvalue problem. For a given point in the $R-\alpha$ plane, and for a given wall inclination ω and a given liquid (the surface tension parameter γ involves only properties of the liquid and the gravitational acceleration), setting the real and imaginary parts of the above-described equation equal to zero yields two simultaneous equations for the eigenvalues of the real and imaginary parts of c . However, since we are interested in curves of neutral stability in the $R-\alpha$ plane, a more useful approach is to specify the imaginary part of c to be zero (which by definition is the case on a neutral-stability curve) and use the eigenvalue equations to solve for α and the real part of c .

The formulation given here is in most respects the same as the formulation of most of the classic problems in hydrodynamic stability. (Boundary conditions (I), (II), and (V), however, are peculiar to this problem because of the free surface.) In particular, the Orr-Sommerfeld equation is the basic equation which invariably governs the streamfunction, and the only obstacle which prevents one from proceeding in a straightforward fashion to the end results is the difficulty involved in finding the general solution to this equation. The usual approach is to expand ϕ in powers of $\frac{1}{\alpha R}$ since, typically, R is quite large. Referring to equation (2.42), one sees that the zeroth-order inviscid equation so obtained (the left hand side equal to zero) has a singularity at the "critical point," defined as the value of y for which $U_0 = c$. Thus, one sees how the difficulties referred to in Section 2.1 can arise.

As indicated in Section 2.1, however, in the present problem

c is always greater than U_0 for small α (for undamped waves, i. e., for the imaginary part of c equal to zero). The kinematic wave theory predicts that, for α tending to zero, c (as nondimensionalized here) tends to three exactly. Equation (2.17), however, shows that the maximum value of U_0 is $3/2$.

On the other hand, the usual procedure of treating $\frac{1}{\alpha R}$ as a small quantity is clearly not valid here, since the experimental results mentioned in Section 2.1 indicate that this quantity is of order one in the region of interest; a new approach must be found.

2.4. Review of Past Attempts to Solve the Problem

The first attempt to find a curve of neutral stability in the R - α plane was made by Yih¹⁹ in 1954. His formulation of the problem was essentially the same as that given in Section 2.3, except that the term corresponding to the one containing the quantity $\frac{\delta}{R^{1/3}}$ in equation (2.44) was omitted. Thus, his analysis pertained only to a fluid with no surface tension. The method used was to treat αR as a small quantity and expand ϕ_i in powers of αR :

$$\phi_i = \phi_i^{(0)} + \alpha R \phi_i^{(1)} + \dots \quad (2.48)$$

Then $\phi_i^{(0)}$ and $\phi_i^{(1)}$ could be found by successive approximations, and the resulting expressions were then used in the boundary conditions (I) through (V). A complicated numerical scheme was used to solve the resulting eigenvalue equations for the case of $\omega = \frac{\pi}{2}$ (a vertical wall). The resulting neutral-stability curve was roughly a C-shaped curve looking very much like the neutral-stability curves

in the classic problems (except for the much lower Reynolds numbers). The minimum value of R on the curve, i. e., the critical value, was about 1.5. (This is not to be compared to experimentally measured values for water, since Yih's analysis was for zero surface tension.) The value of αR at the critical point was between 1.1 and 1.2, and ϕ_1'' was of the order of a half or more of ϕ_1'' except when y was close to zero ($\phi_1'''(0) = 0$), so the expansion indicated in equation (2.48) was at best a very slowly converging series. In addition, the limiting value of c as α tended to zero was greater than twelve, contradicting the kinematic-wave result.

Benjamin¹ attacked the problem in 1957, and his remains the major contribution. He successfully demonstrated for the first time that the characteristics of the neutral-stability curves were quite different from the classical shapes.

His formulation of the problem was essentially equivalent to that given here (including the term containing the surface tension parameter γ). His approach was to look for a solution for ϕ_1 in the form of a power series in y :

$$\phi_1 = \sum_{n=0}^{\infty} A_n y^n.$$

The recursion relationship for the A_n 's shows that for large n they are given as increasing powers of α^2 and αR . Benjamin treats both α^2 and αR as small parameters (of the same order) and truncates the series accordingly. The boundary conditions, of course, are also expanded in powers of α^2 and αR . Since in equation (2.44) the term containing the surface tension parameter also involves

$R^{-1/3}$, it may be expected that an expansion in powers of α^2 and αR would cause difficulties. Benjamin's approach is to carry the quantity $\frac{\gamma}{R^{1/3}}$ along throughout the analysis, essentially treating it as a constant.

The resulting neutral-stability curves, for different values of γ , were shown to be curves of positive slope that intersect at a point on the R -axis. (One should expect surface tension to be of no importance as α tends to zero.) The point of intersection, which marks the critical Reynolds number as long as the curves never turn back to lower values of R at some point far from the R -axis, was shown to be given by the relation

$$R_{int} = \frac{5}{6} \cot \omega \quad (2.49)$$

Since α^2 and αR are both zero as α tends to zero, equation (2.49) is an exact result.

The important consequence of equation (2.49) was that for a vertical wall ($\omega = \frac{\pi}{2}$) the curves merge at the origin, indicating the surprising result that there exist unstable wavelengths at all Reynolds numbers. Benjamin also performed a very approximate calculation which showed that amplification rates were very small at the low Reynolds numbers, thus accounting for the difficulty in detecting waves at very low values of R . Although his approximations are valid only in a small neighborhood of the R -axis, his demonstration of the fact that the neutral-stability curves for a vertical wall merge at the origin, where his approximations are indeed valid, was a very significant result.

For the case of a vertical wall and zero surface tension (the case studied by Yih in 1954), Benjamin's results indicated an apparent neutral-stability curve which was essentially a horizontal line at α equal to .44. He includes it as a dotted line in his graph of the neutral-stability curves, and concludes that "the values of α in this case are rather too large for confidence in the accuracy of the result."

It should also be noted that in the limit of small α his solutions indicate a value of c equal to three, in agreement with the kinematic-wave theory prediction.

In 1963, Yih²⁰ returned to the problem and considered the asymptotic behavior of the solution to the Orr-Sommerfeld equation in several limiting cases, all of which he treated with a method of successive approximations essentially the same as he had used in 1954. His goal in this paper, however, is to deduce the general features of the neutral-stability curves by finding the sign of the imaginary part of c in various regions in the R - α plane; no attempt is made to obtain quantitative results for the neutral-stability curves themselves.

For the case of α very small, the analysis is a little less complicated than that which results by only taking the product αR to be small, since, for example, the zeroth-order equation is now

$$\frac{d^4 \phi_1^{(0)}}{dy^4} = 0. \quad (2.50)$$

He is able to reproduce Benjamin's result that the neutral-stability

curves branch out from the R-axis at a point R_{int} given by equation (2.49).

For the case of the product αR small, he obtains zeroth- and first-order equations for ϕ_1'' and ϕ_1''' identical to those obtained in his 1954 paper. His analysis follows very closely that given in 1954 except that the term containing $\frac{\gamma}{R^{1/3}}$ is now included in boundary condition (II). The analysis, of course, is valid only if the product αR is small, but by considering vanishingly small values of R he attempts to find the sign of the imaginary part of c at arbitrarily large values of α .

The term containing $\frac{\gamma}{R^{1/3}}$ is treated in much the same way as Benjamin handled it; it is factored out and regarded as a constant which cannot be dropped. There is, however, an important difference in the two approaches. Since Yih's result is to be applied to the case of large α , his zeroth-order solution must pertain to the case of zero Reynolds number (for any assumed value of γ). Thus, $\frac{\gamma}{R^{1/3}}$ is constant only if γ is proportional to $R^{1/3}$, but γ is considered to be a constant. Yih's approach therefore becomes an attempt to expand ϕ_1 about a singular point at $R = 0$ implied by condition (II). Thus it follows that the dependence on γ of the resulting expression for the imaginary part of c will not be correct. Using these results, however, he finds that the general qualitative features of Benjamin's curves appear to be correct.

Yih uses the expression for the imaginary part of c at large α in returning to the case of zero surface tension and a vertical wall. By setting γ equal to zero and ω equal to $\frac{\pi}{2}$, he obtains

an expression which is assumed to be valid for very large α and vanishingly small \mathcal{R} . Using asymptotic expansions appropriate to the case of large α for the functions of α involved, he finds the imaginary part of c to be positive, thus implying the flow is unstable at large α . Since it is also unstable at low α , he concludes it is probably unstable at intermediate values, and the entire first quadrant is a region of instability.

In his book, Dynamics of Nonhomogeneous Fluids²¹, however, Yih reveals that there was an algebraic error involved in finding the sign of the expression for the imaginary part of c at large α ; he now finds it to be negative. Thus, he necessarily concludes that since there is a positively damped (stable) region at large α , there must be a neutral-stability curve (similar to the dotted line tentatively suggested in Benjamin's curves) at some intermediate value. This proof, however, is highly questionable for the reasons indicated above, and, in fact, an alternate proof to the contrary is given in Section 2.7.

2.5. The Present Solution

As indicated earlier, the usual approach to the Orr-Sommerfeld equation is to make use of the fact that $\alpha\mathcal{R}$ is a large quantity. All attempts to solve the current problem have also used $\alpha\mathcal{R}$ as the primary expansion parameter, usually taken to be small rather than large. We note, however, that the difficulty in solving the Orr-Sommerfeld equation arises from the non-constant coefficient $(c - U_0)$. But since c is of the order of three for long waves, the

y-dependence of $(c - U_0)$ is a relatively weak one. (U_0 varies between 0 and 3/2.) Thus a simple and straightforward first approximation may be obtained by replacing $(c - U_0)$ by its average value $(c - 1)$. The domain of validity in the R - α plane of the solutions which result from this approximation will be estimated after the solutions are obtained.

With this approximation, the general solution to equation (2.42) is readily found to be

$$\phi_1(y) = A_1 e^{\lambda_1 y} + B_1 e^{-\lambda_1 y} + A_2 e^{\lambda_2 y} + B_2 e^{-\lambda_2 y}, \quad (2.51)$$

where

$$\lambda_1 = \left\{ \left(\alpha^2 + \frac{g}{2} \right) + i \left(-\frac{\alpha R}{2} (c-1) + \frac{3\alpha R}{g} \right) \right\}^{1/2}, \quad (2.52)$$

$$\lambda_2 = \left\{ \left(\alpha^2 - \frac{g}{2} \right) + i \left(-\frac{\alpha R}{2} (c-1) - \frac{3\alpha R}{g} \right) \right\}^{1/2}, \quad (2.53)$$

and in which

$$g = \left\{ -\frac{1}{2} \alpha^2 R^2 (c-1)^2 + \frac{1}{2} \sqrt{\alpha^4 R^4 (c-1)^4 + (144) \alpha^2 R^2} \right\}^{1/2} \quad (2.54)$$

In equation (2.51), A_1 , A_2 , B_1 , and B_2 , are, of course, unknown constants of integration.

If we use this expression in the five boundary conditions and set the determinant of the coefficients equal to zero, we obtain the following complex eigenvalue equation:

$$K_1 K_4 = K_2 K_3 \quad (2.55)$$

in which

$$K_1 = \lambda_1 e^{\lambda_1} - \frac{1}{2} \lambda_2 e^{\lambda_2} (\lambda_1 + \lambda_2) + \frac{1}{2} \lambda_2 e^{-\lambda_2} (\lambda_1 - \lambda_2) +$$

$$+ \frac{(\alpha^2(c - \frac{3}{2}) - 3)}{c - \frac{3}{2}} \left[e^{\lambda_1} - \frac{\lambda_1}{\lambda_2} \sinh \lambda_2 - \cosh \lambda_2 \right], \quad (2.56)$$

$$K_2 = \lambda_1 e^{-\lambda_1} + \frac{1}{2} \lambda_2 e^{\lambda_2} (\lambda_1 - \lambda_2) - \frac{1}{2} \lambda_2 e^{-\lambda_2} (\lambda_1 + \lambda_2) +$$

$$+ \frac{(\alpha^2(c - \frac{3}{2}) - 3)}{c - \frac{3}{2}} \left[e^{-\lambda_1} + \frac{\lambda_1}{\lambda_2} \sinh \lambda_2 - \cosh \lambda_2 \right], \quad (2.57)$$

$$K_3 = \lambda_1 e^{\lambda_1} (\lambda_1^2 - S) - \frac{1}{2} (\lambda_2^2 - S) (\lambda_1 + \lambda_2) e^{\lambda_2} -$$

$$- \frac{1}{2} (\lambda_2^2 - S) (\lambda_1 - \lambda_2) e^{-\lambda_2} -$$

$$- \frac{\left(3i\alpha \cot \omega + \frac{i\alpha^3 \delta}{R^{2/3} (\sin \omega)^{1/3}} \right)}{c - \frac{3}{2}} \left[e^{\lambda_1} - \frac{\lambda_1}{\lambda_2} \sinh \lambda_2 - \cosh \lambda_2 \right], \quad (2.58)$$

$$K_4 = -\lambda_1 e^{-\lambda_1} (\lambda_1^2 - S) + \frac{1}{2} (\lambda_2^2 - S) (\lambda_1 - \lambda_2) e^{\lambda_2} +$$

$$+ \frac{1}{2} (\lambda_2^2 - S) (\lambda_1 + \lambda_2) e^{-\lambda_2} -$$

$$- \frac{\left(3i\alpha \cot \omega + \frac{i\alpha^3 \delta}{R^{2/3} (\sin \omega)^{1/3}} \right)}{c - \frac{3}{2}} \left[e^{-\lambda_1} + \frac{\lambda_1}{\lambda_2} \sinh \lambda_2 - \cosh \lambda_2 \right], \quad (2.59)$$

where

$$S = 3\alpha^2 - i\alpha R(c - \frac{3}{2}) \quad (2.60)$$

Assuming c is real, equation (2.55) can be separated into its real and imaginary parts, and for any given R (and δ and ω) the solutions for α and c can be found. Using the IBM 7094 computer, solutions have been found for the three wall angles corresponding to $\omega = 90^\circ$, 60° , and 30° . Figures 7, 8, and 9 give the resulting curves of neutral stability, and Figures 10, 11, and 12 show the solutions for c , corresponding to the neutral-stability curves. We note that as α tends to zero, c tends exactly to three, as predicted by the kinematic-wave theory.

In Figures 7, 8, and 9, Benjamin's solutions have been plotted for comparison. The data points for Benjamin's curves have been computed using his equation (4.13), but an apparent typographical sign error on the last term in the equation has been corrected. (Without this change, the resulting curves are radically different from the curves Benjamin has drawn in his Figure 2; with the sign change the curves and the equation are in perfect agreement.)

In Figures 7, 8, and 9, the region below each curve corresponds to a positive value for the imaginary part of c (i.e., negative damping) and thus is a region of instability. Similarly, the region above the curves is a region of stability. As is reasonable, increasing the value of the surface tension parameter δ is seen to have a stabilizing effect.

The solutions given are based on the assumption that $(c - U_\infty)$

is approximately equal to $(c-1)$. The per cent error, relative to the exact expression $(c-u_0)$ is given by $\bar{\kappa}$:

$$\bar{\kappa} = 100 \left(\frac{c-1}{c-u_0(y)} - 1 \right) \quad (2.61)$$

Using the expression for u_0 given by equation (2.17), and integrating from 0 to 1, we find the average value of $\bar{\kappa}$ to be:

$$\bar{\kappa} = 100 \left[\frac{\sqrt{\frac{2}{3}} (c-1)}{\sqrt{c-\frac{3}{2}}} \tan^{-1} \left\{ \frac{\sqrt{\frac{3}{2}}}{\sqrt{c-\frac{3}{2}}} \right\} - 1 \right] \quad (2.62)$$

In Figure 13, the variation of $\bar{\kappa}$ with c is indicated graphically. The dependence of $\bar{\kappa}$ on c is seen to be relatively weak for c greater than about 2.4, and the accuracy of the resulting neutral-stability curves may be expected to be relatively independent of the solutions for c if c is between 3.0 (its maximum value) and about 2.4.

Benjamin's solutions should be very accurate for very small values of α (they are exact in the limit as α tends to zero), and the present solutions are in extremely good agreement with Benjamin's for the case of small α . Referring to Figures 7 through 13, it is clear that the present solutions may be expected to give a quantitatively useful representation of the neutral-stability curves up to values of α on the order of 0.8 (which roughly corresponds to values of c on the order of 2.2 or 2.3, or values of $\bar{\kappa}$ on the order of 10 to 15 per cent, compared with 5 per cent when α equals zero and c equals 3). In contrast, it is clear from Figures 7, 8, and 9 that Benjamin's solutions break down for values of α on the order

of 0.3 .

A few of the neutral-stability curves in Figures 7, 8, and 9 have been extended to values of α as large as 1.0 to indicate the general trends, but these points, which correspond to values of c of about 2.0 and values of $\bar{\delta}$ of about 20 per cent, are of questionable accuracy.

2.6 Energy Conservation

The points on the neutral-stability curves correspond to undamped wave motion. Since energy is continuously being removed due to viscous dissipation, the question arises as to what is the source of energy input into the flow and what is the role played by gravity in this process. The energy input cannot come directly from gravitational effects, since the first-order Navier-Stokes equations, equations (2.22) and (2.23), are independent of gravity. (Gravitational effects are completely accounted for by the zeroth-order flow.) In fact, one is led to suspect from this that gravity plays no role in the stability problem, that is, that the analysis is exactly the same if one considers the stability of a film whose given velocity profile (in the absence of gravity) just happens to be that given by equation (2.17). (We may consider a vertical wall, so equation (2.18) is also satisfied.) Of course, this zeroth-order flow will decay with time in the absence of gravity, but if the characteristic relaxation time is long compared to a characteristic time associated with the wave propagation, this will not be an important effect.

In fact, however, this is not the case. If one considers the

parallel laminar flow without gravity, the equation of motion becomes

$$\frac{\partial u^*}{\partial t^*} = \nu \frac{\partial^2 u^*}{\partial y^{*2}} \quad (2.63)$$

The solution which satisfies the boundary conditions is

$$u^* = \sum_{n=1}^{\infty} A_n e^{-\frac{\nu(n-\frac{1}{2})^2 \pi^2}{(h_0^*)^2} t^*} \sin \frac{(n-\frac{1}{2}) \pi y^*}{h_0^*}, \quad (2.64)$$

where the A_n 's are the appropriate Fourier coefficients in the expansion of the initial velocity profile. Since we are considering a parabolic profile given by equation (2.17), the first eigensolution is clearly the dominant one. It has a characteristic relaxation time t_r^* given by

$$t_r^* = \frac{4h_0^{*2}}{\nu \pi^2},$$

or, non-dimensionalizing,

$$t_r = \frac{4}{\pi^2} R.$$

On the other hand, the characteristic time t_λ^* for a wave crest to travel a distance of one wavelength is, non-dimensionalized,

$$t_\lambda = \frac{2\pi}{\alpha c}.$$

At a typical solution point we have, say, R equal to 5.0, α equal to .3, and c equal to 3.0. Then t_r is of the order of 2 and t_λ is of the order of 7. Clearly, t_r is not large compared to t_λ . Thus, gravity plays a vital role, even though it enters the problem directly only at the zeroth order.

It follows that there must exist some mechanism by which

energy is diverted from the zeroth-order flow into the first-order disturbance motion. This mechanism becomes apparent from an examination of the first-order equation of motion for u_1 , given by equation (2.22). Since U_1'' is zero, this becomes

$$\frac{\partial u_1}{\partial t} + U_0 \frac{\partial u_1}{\partial x} = - \frac{\partial p_1}{\partial x} + \frac{1}{R} \nabla^2 u_1 - U_0' v_1. \quad (2.65)$$

The term $U_0' v_1$ has been placed on the right side since it is not part of the Eulerian derivative of u_1 . Using the continuity relation of equation (2.19) and noting that U_0 is not a function of x , this term may be written

$$- U_0' v_1 = \frac{\partial}{\partial x} (-U_0 u_1) + \frac{\partial}{\partial y} (-U_0 v_1).$$

Thus we see that u_1 is acted upon by a normal stress, $-U_0 u_1$, and a shear stress, $-U_0 v_1$, (similar to the Reynolds stresses that arise from turbulent disturbances) which arise from the interaction of the zeroth-order and the first-order flows. This, then, provides the mechanism by which energy can be diverted into the wave disturbance (at a large enough rate to balance the loss due to dissipation).

2.7 The Case of a Vertical Wall and a Liquid Without Surface Tension.

We now consider the case of $\omega = \frac{\pi}{2}$ and $\gamma = 0$. It should be noted under these conditions there do exist solutions to equation (2.55), but the values of c associated with these solutions are between 1.78 and 1.8, and Figure 13 indicates that such values of c are too low for the solution to have significance.

We shall assume that there exists an undamped wave, for which c is greater than 3/2 (this is the case considered by Yih), and

examine the consequences of that assumption. We now choose a coordinate system that travels with the wave at speed c , as indicated in Figure 14. In this coordinate system we have a steady-state flow field, and the wall travels upward with speed c . The coordinate system has been chosen so that x is zero at a point of maximum thickness. Thus,

$$\eta_1 = \Theta_1 \cos \alpha x . \quad (2.66)$$

It is clear that, to be consistent with this, the streamfunction must vary like a cosine also:

$$\psi_1 = \phi_1 \cos \alpha x . \quad (2.67)$$

Thus the velocity components are

$$u_1 = \phi_1' \cos \alpha x , \quad (2.68)$$

$$v_1 = \alpha \phi_1 \sin \alpha x . \quad (2.69)$$

To first order, the slope of a streamline is given by

$$\frac{dy}{dx} = \frac{v_1}{U_0} + O(\Theta_1^2) = \frac{\alpha \phi_1}{U_0} \sin \alpha x + O(\Theta_1^2) , \quad (2.70)$$

and the curvature, to the first order, becomes

$$\frac{d^2y}{dx^2} = \frac{\alpha^2 \phi_1}{U_0} \cos \alpha x + O(\Theta_1^2) . \quad (2.71)$$

As we move along the y -axis from the surface toward the wall, we must reach a point y_s where the curvature goes to zero, as indicated in Figure 14. (The curvature must be zero at the wall, so y_s may be zero. However, if there exists a node in the flow, y_s may be greater than zero.) We note that we must have $\phi_1(y_s)$ equal to zero. This means that at $y = y_s$ the curvature and the y -

component of velocity are zero for all x ; the streamline at $y = y_s$ is straight and parallel to the wall, as shown in the figure.

We shall now restrict our attention to the streamtube bounded by the free surface and the streamline at $y = y_s$, and we wish to consider the change in u , which takes place along any streamline in that streamtube between station 1 and station 2, a half-wavelength away.

In this coordinate system, the first-order equation of motion (cf. equation (2.65)) is

$$U_0 \frac{\partial u_1}{\partial x} = - \frac{\partial p_1}{\partial x} + \frac{1}{R} \nabla^2 u_1 - U_0' v_1 . \quad (2.72)$$

We note that the total rate of change of a quantity with respect to x along a streamline is given by

$$\frac{d}{dx} = \frac{\partial}{\partial x} + \frac{\partial}{\partial y} \frac{dy}{dx} ,$$

but since $\frac{dy}{dx}$ is a first-order quantity, as indicated by equation (2.70), we have

$$\frac{d}{dx} = \frac{\partial}{\partial x} + O(\theta_1) . \quad (2.73)$$

Thus, equation (2.72) becomes

$$U_0 \frac{du_1}{dx} = - \frac{dp_1}{dx} + \frac{1}{R} \nabla^2 u_1 - U_0' v_1 + O(\theta_1^2) .$$

Integrating from station 1 to station 2 along a streamline, characterized by, say, $y = y_s$, as indicated in Figure 14, we find

$$U_0 \Delta_{1,2} u_1 = -\Delta_{1,2} p_1 + \frac{1}{R} \int_{st.1}^{st.2} (\nabla^2 u_1) dx - \int_{st.1}^{st.2} (U_0' u_1) dx + O(\Theta^2) , \quad (2.74)$$

where $\Delta_{1,2}$ indicates the value of a quantity at station 2 minus its value at station 1.

We shall consider the terms of order Θ , on the right side of equation (2.74) individually. We note that at station 1 all the fluid in the streamtube being considered has an acceleration vector pointing towards the wall. There are only two possible sources for the forces which produce those accelerations: stress gradients and pressure gradients. The stress gradients which act in the y-direction are proportional to $\nabla^2 u_1$. We see from equation (2.69), however, that at $x = 0$ we must have $\nabla^2 u_1 = 0$. Thus, the acceleration is solely the result of the pressure distribution. It follows that the pressure profile must be as indicated in Figure 14 (atmospheric pressure is still taken to be zero). Thus, at station 1 the pressure is necessarily negative in the streamtube considered. A similar argument shows the pressure to be positive at station 2. Thus, $\Delta_{1,2} p_1$ is a positive quantity, or

$$-\Delta_{1,2} p_1 < 0 .$$

Considering the second term on the right of equation (2.74) we note that $\nabla^2 u_1$ is a function of both x and y , both of which vary along the streamline. However, as we have shown, to the lowest

order the y-variation along the streamline may be neglected. Thus, from equation (2.68) we see that $\nabla^2 u_1$ is proportional to $\cos \alpha x$ and thus its integral from station 1 to station 2 (i.e., from $x = 0$ to $x = \frac{\pi}{\alpha}$) must vanish. That is to say

$$\frac{1}{R} \int_{\text{st. 1}}^{\text{st. 2}} (\nabla^2 u_1) dx = 0 + O(\epsilon_1^2)$$

We now note that between station 1 and station 2 both U_0' and u_1 are negative. Thus

$$- \int_{\text{st. 1}}^{\text{st. 2}} (U_0' u_1) dx < 0$$

We therefore conclude that equation (2.74) implies that

$$\Delta_{1,2} u_1 < 0,$$

that is, the x-component of the velocity decreases along every streamline in the streamtube in traveling from station 1 to station 2. Since the streamtube thickness is less at station 2 than station 1, it follows that the mass flow rate is less at station 2 than station 1. Thus, the continuity equation is violated.

Thus we see that for $\omega = \frac{\pi}{2}$ and $\gamma = 0$ waves of the type predicted by Yih, and tentatively suggested by Benjamin, cannot in fact exist on simple physical grounds; the momentum and continuity equations cannot be satisfied simultaneously.

2.8 Concluding Remarks

It should be noted that the neutral-stability curves given in Figures 7, 8, and 9 are based on an approximate method of solution of the Orr-Sommerfeld equation which is fundamentally different from the approach used by Benjamin. The remarkably good agreement which results at small values of α thus serves to confirm the validity of both approaches. (Benjamin's solutions are valid over a much smaller domain than those presented here, although they have the advantage of being obtained analytically, rather than numerically.)

Yih's²⁰ recent approach, on the other hand, has been shown to be unsatisfactory. He considers separately the case of small α and the case of small R . In the latter case, his approach becomes an attempt to expand a function of R in a Taylor series about a singular point of that function. In this way he is led to the erroneous conclusion that there exists a neutral-stability curve in the R - α plane for the case of zero surface tension and a vertical wall. It has been shown here that the undamped waves which would correspond to the points on such a curve are not physically possible.

It should be noted that the emphasis here has been on finding the neutral-stability curves, i. e., finding α (and c) as a function of R when the imaginary part of c is zero. If information about the amplification rates is desired, equation (2.55) may equally well be used to find, for example, both the real and imaginary parts of c for given values of α and R .

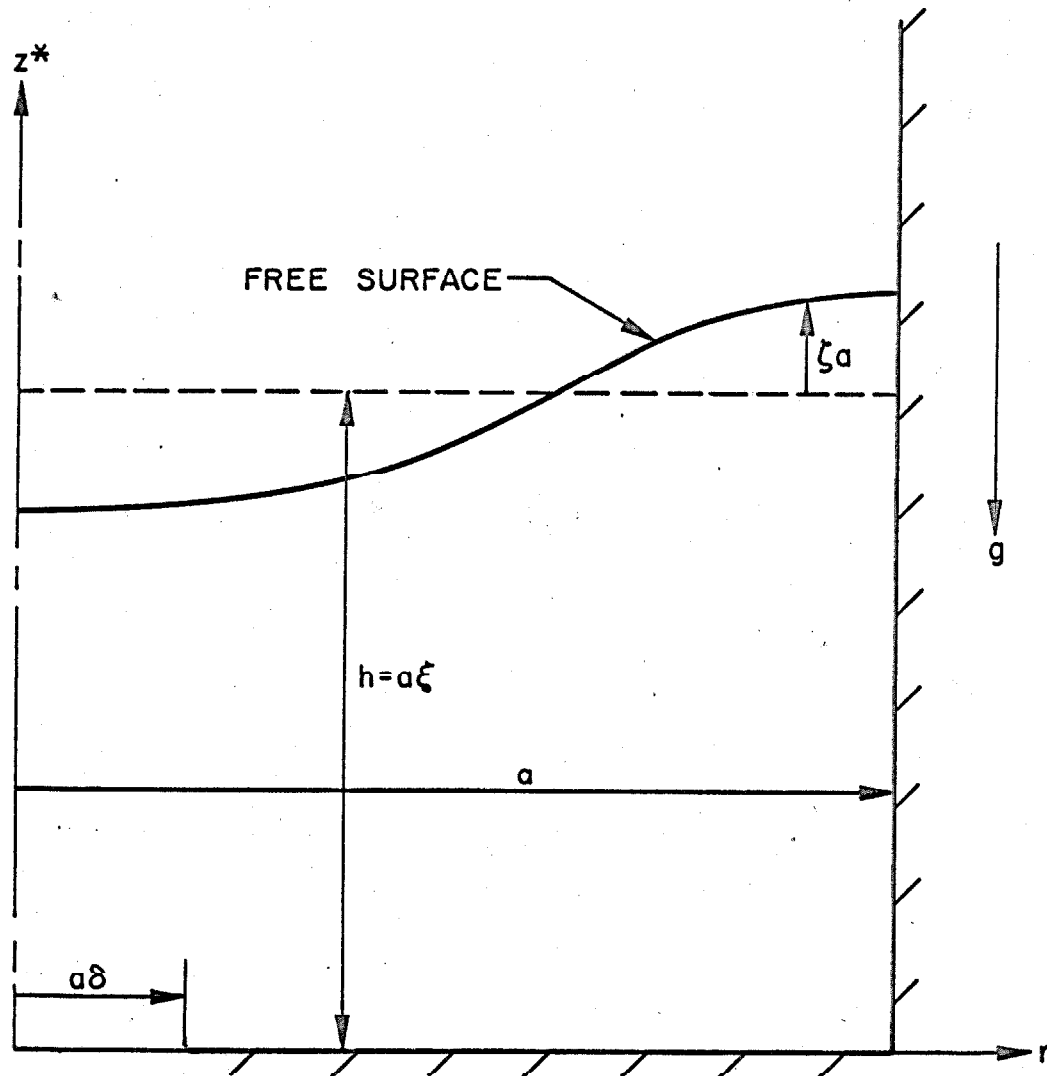


FIGURE 1: DEFINITION SKETCH FOR PART I

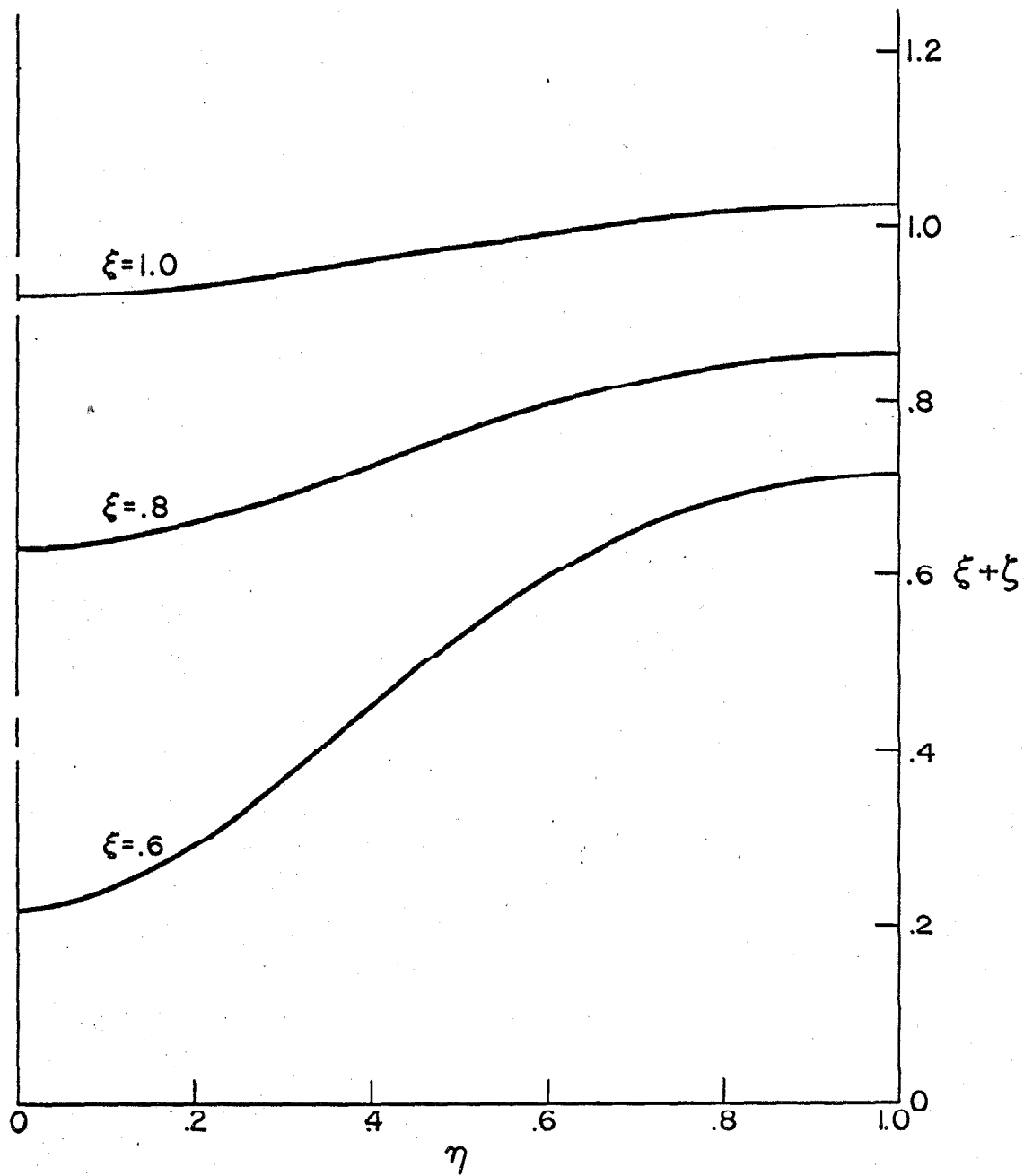


FIGURE 2: SURFACE PROFILES
FOR $\delta \rightarrow 0$
($\xi_0 \rightarrow \infty$, $F \rightarrow \infty$)

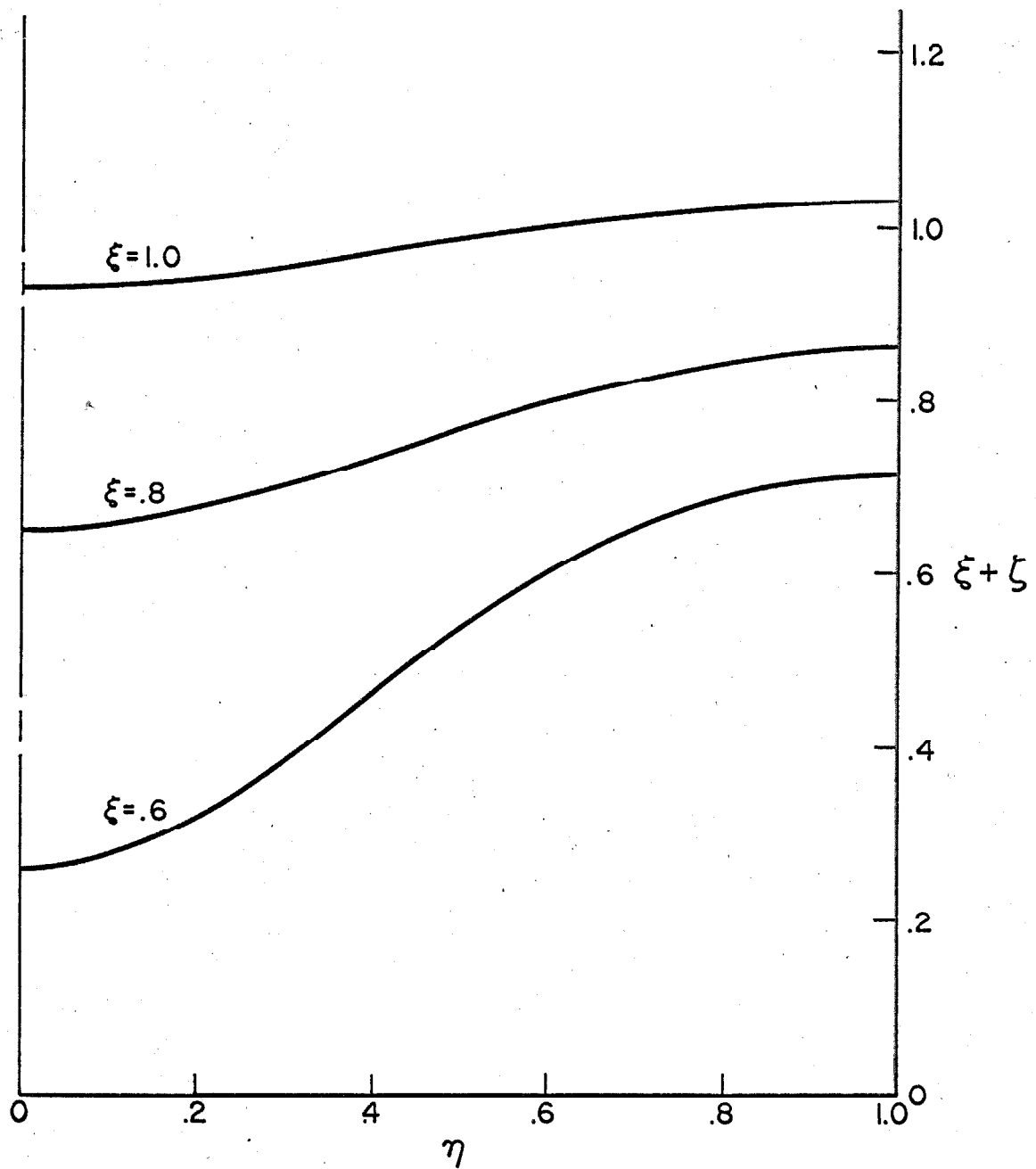


FIGURE 3: SURFACE PROFILES
FOR $\delta = .2$
($\xi_0 \rightarrow \infty$, $F \rightarrow \infty$)

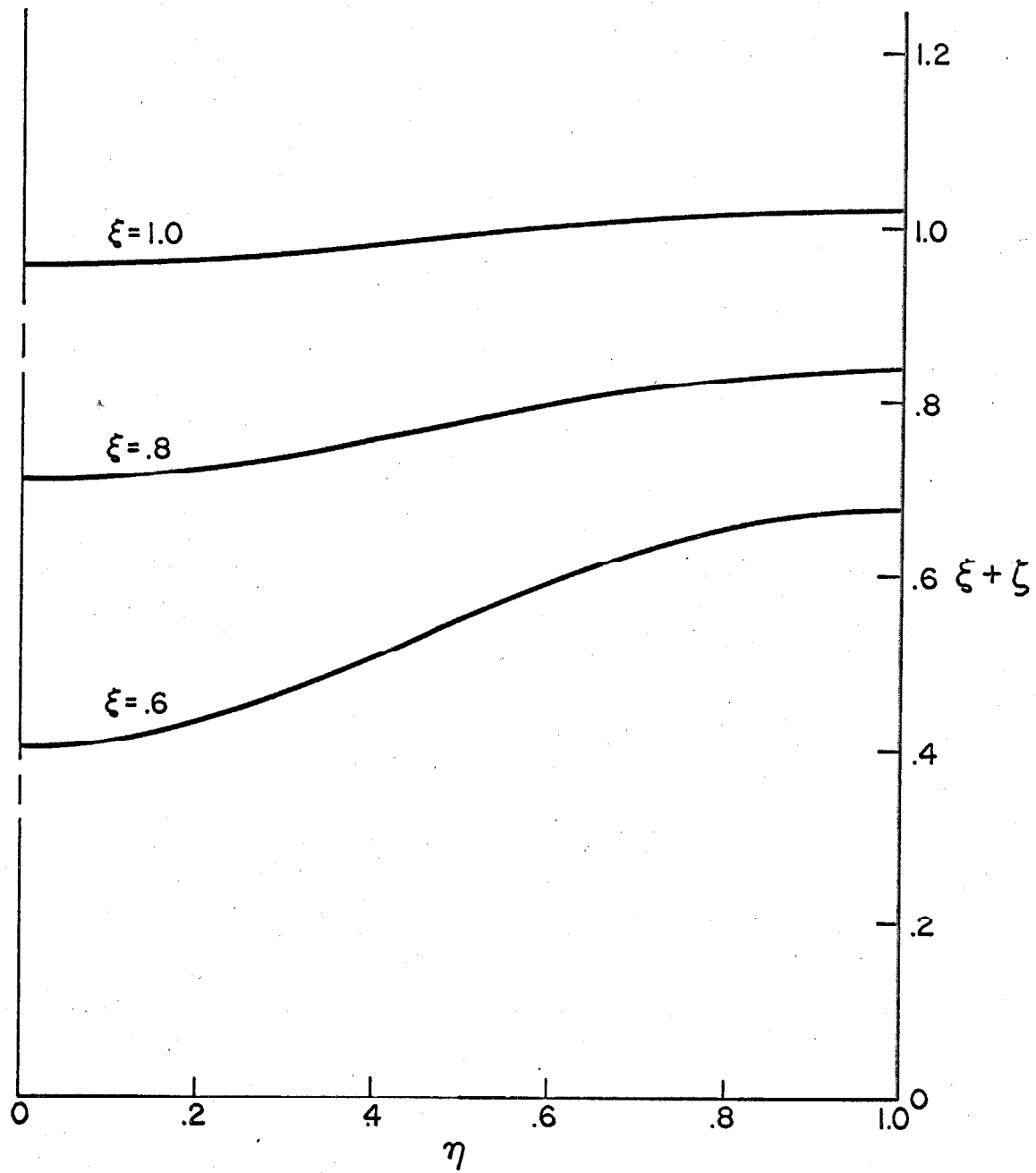


FIGURE 4: SURFACE PROFILES
FOR $\delta = .5$
($\xi_0 \rightarrow \infty$, $F \rightarrow \infty$)

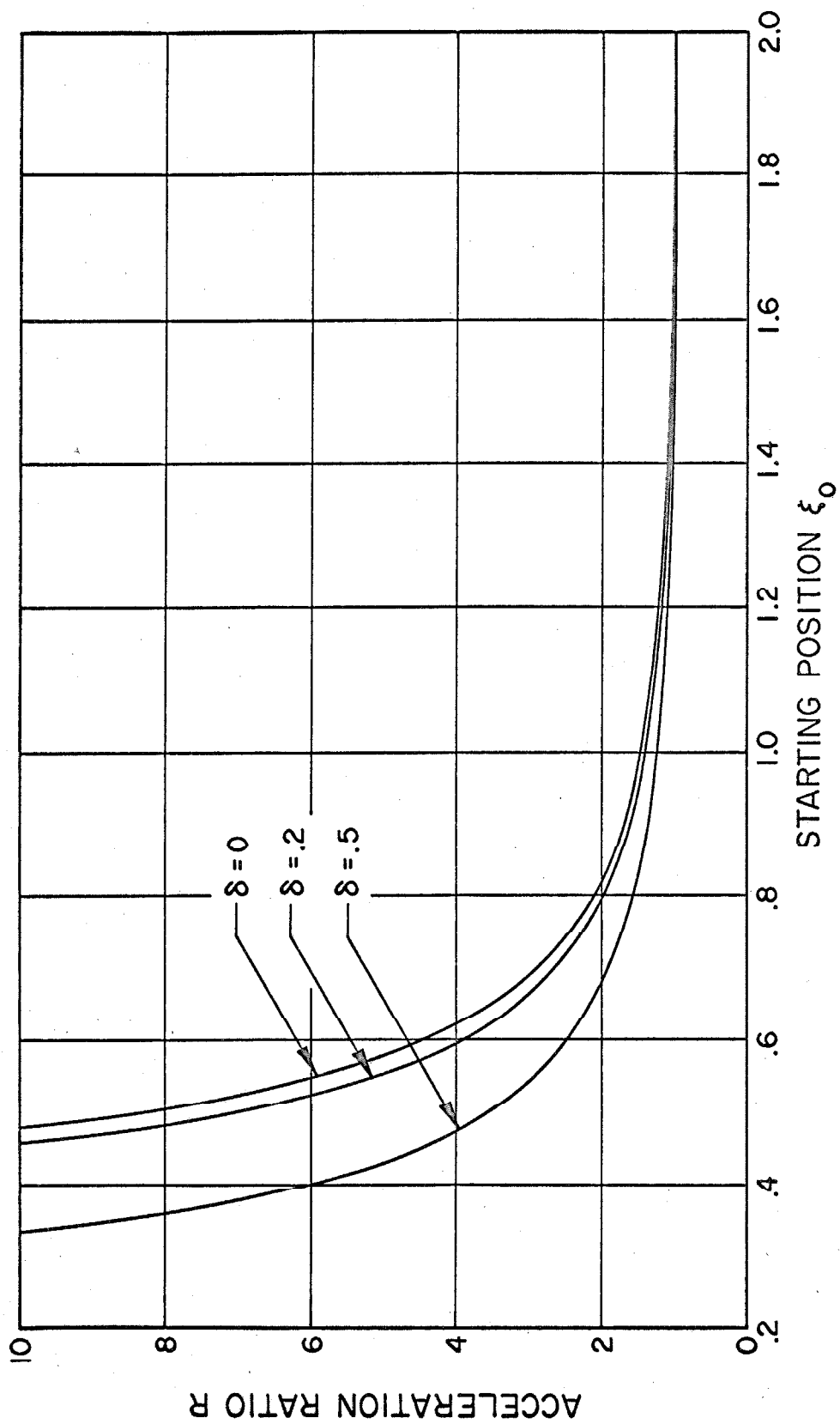


FIGURE 5: RATIO OF INITIAL ACCELERATION OF THE FREE SURFACE AT THE CENTER TO THAT AT THE WALL

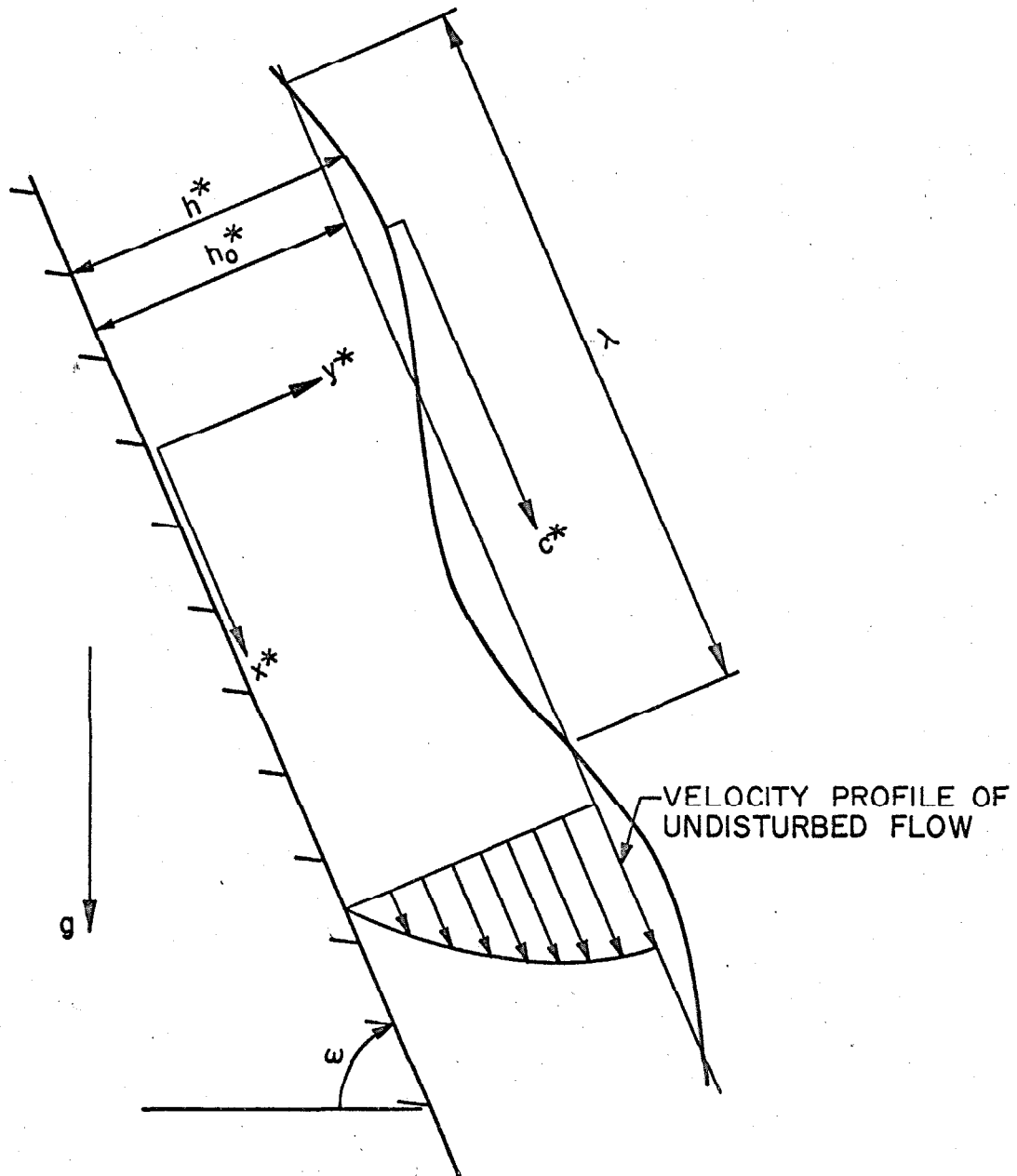


FIGURE 6: DEFINITION SKETCH FOR PART II

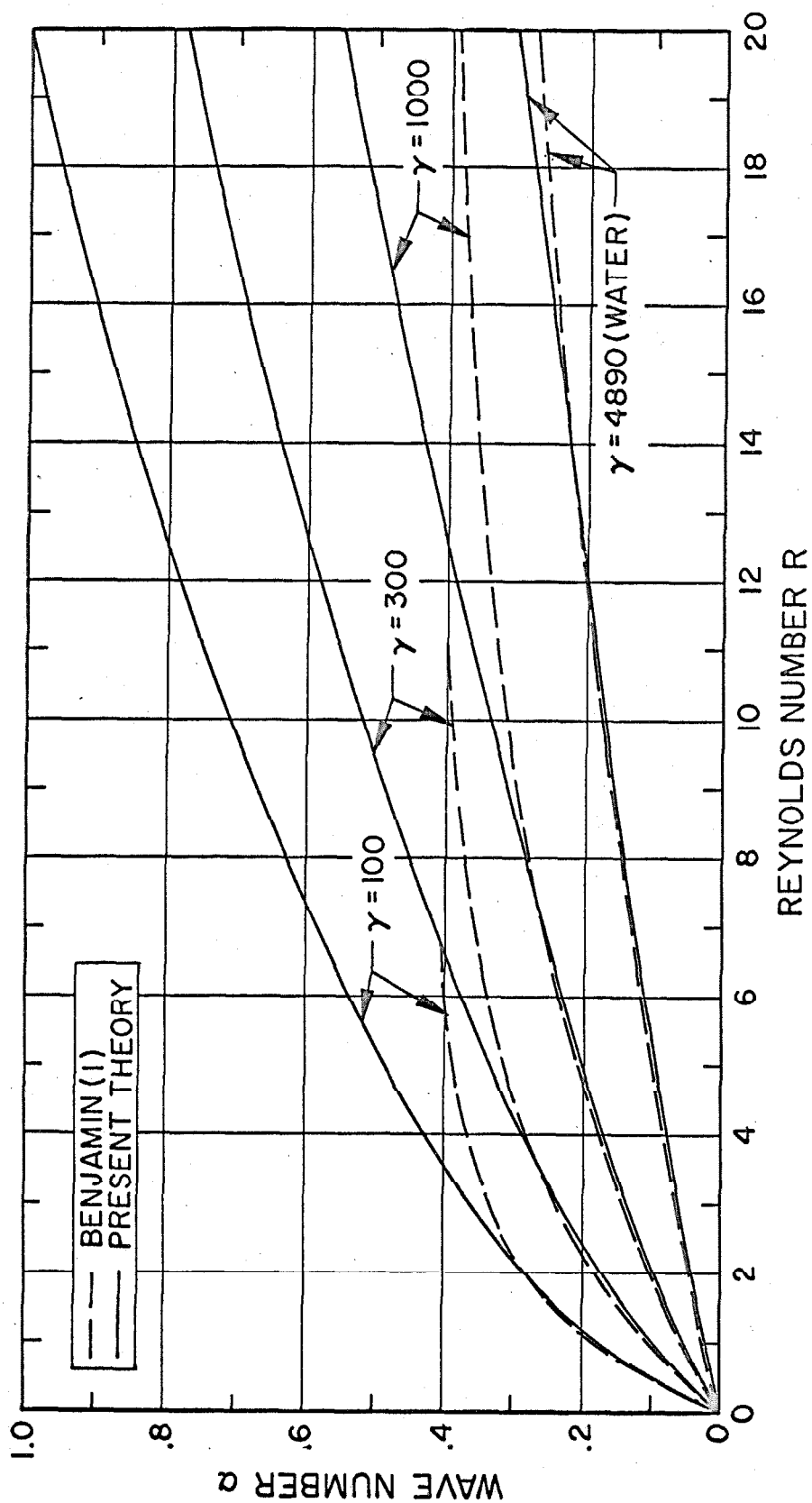


FIGURE 7: CURVES OF NEUTRAL STABILITY FOR $\omega = 90^\circ$

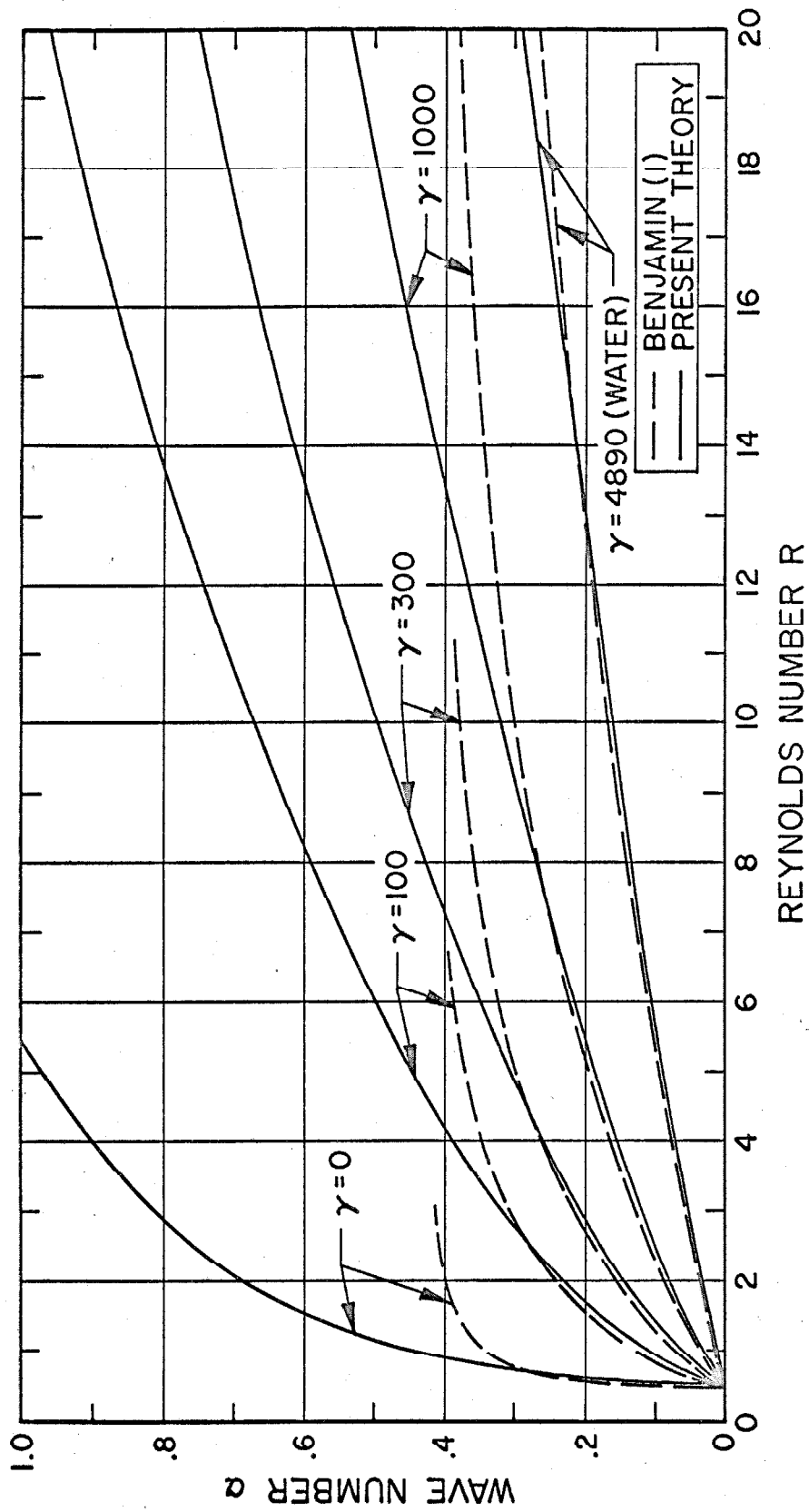


FIGURE 8: CURVES OF NEUTRAL STABILITY FOR $\omega = 60^\circ$

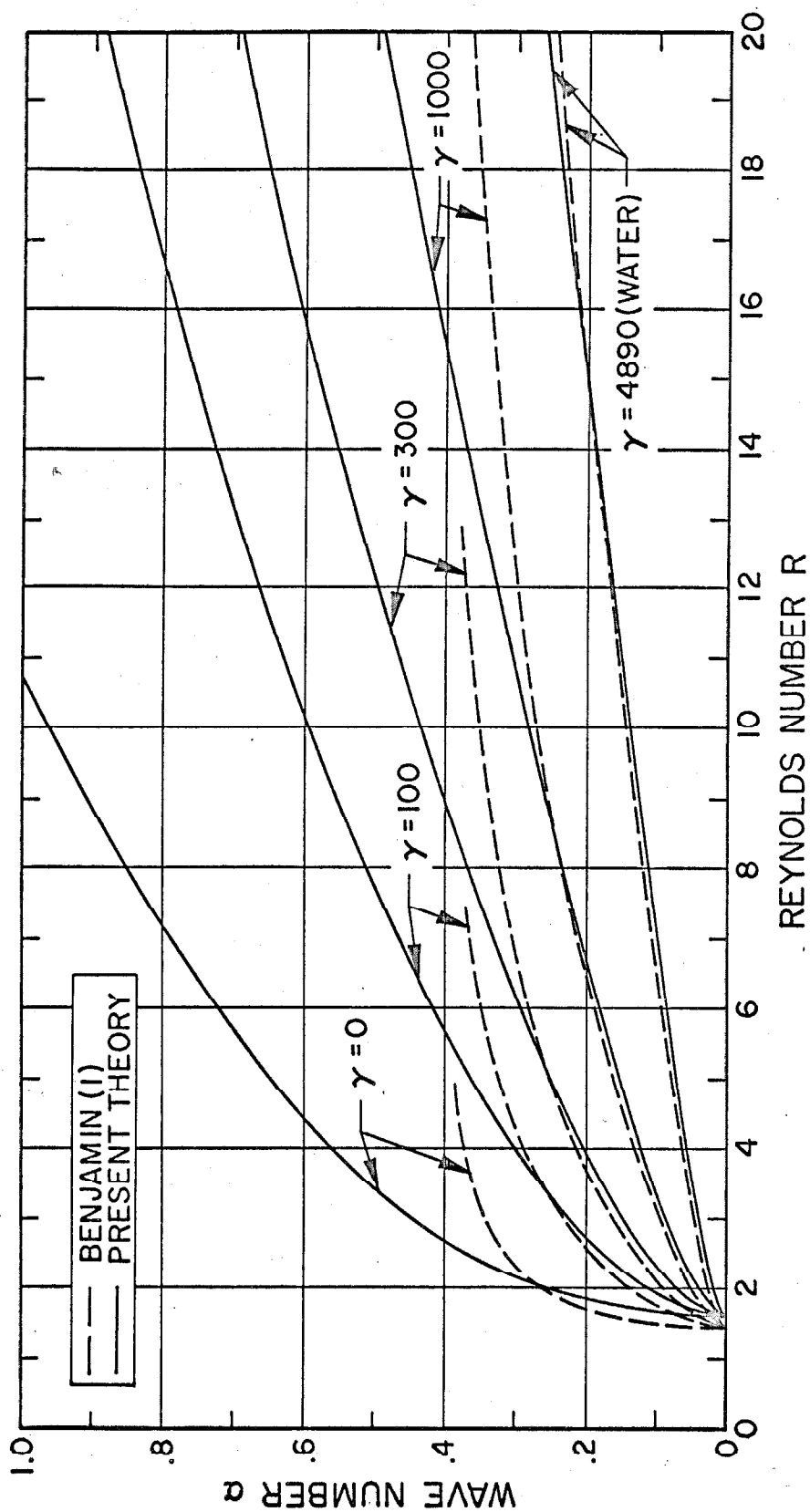


FIGURE 9: CURVES OF NEUTRAL STABILITY FOR $\omega = 30^\circ$

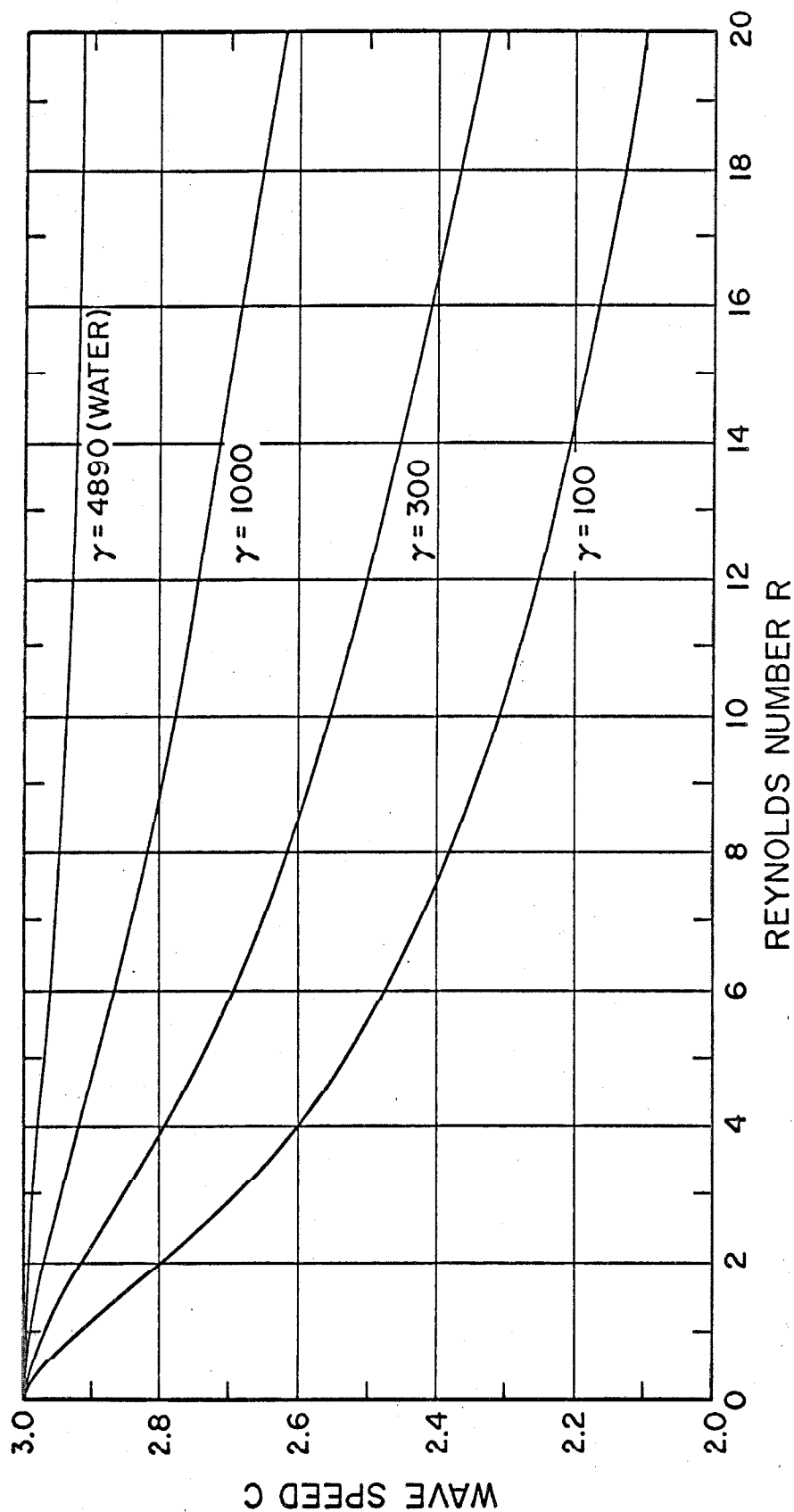


FIGURE 10: VARIATION OF WAVE SPEED WITH REYNOLDS NUMBER ON NEUTRAL - STABILITY CURVES FOR $\omega = 90^\circ$

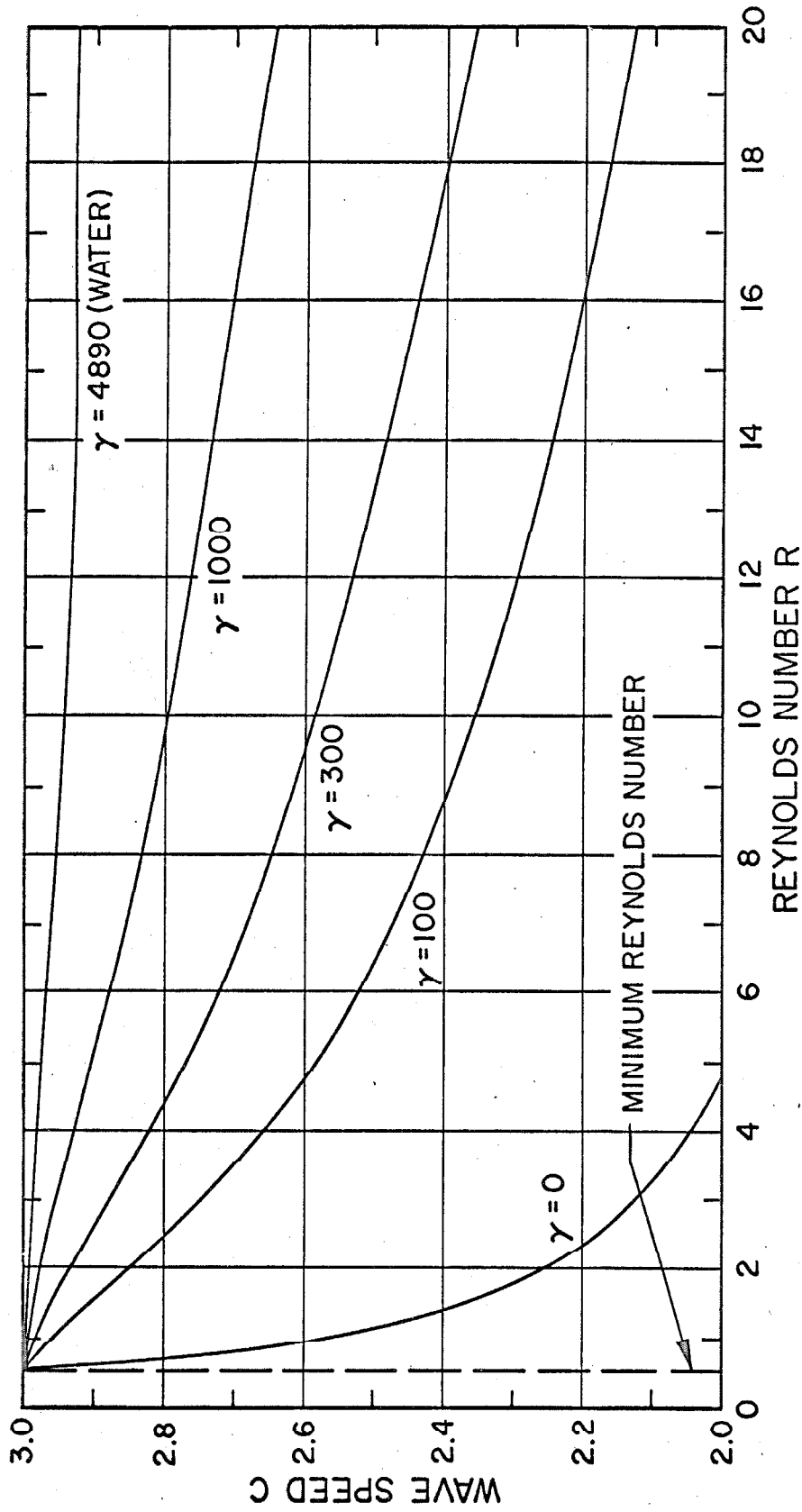


FIGURE II: VARIATION OF WAVE SPEED WITH REYNOLDS NUMBER
ON NEUTRAL - STABILITY CURVES FOR $\omega = 60^\circ$

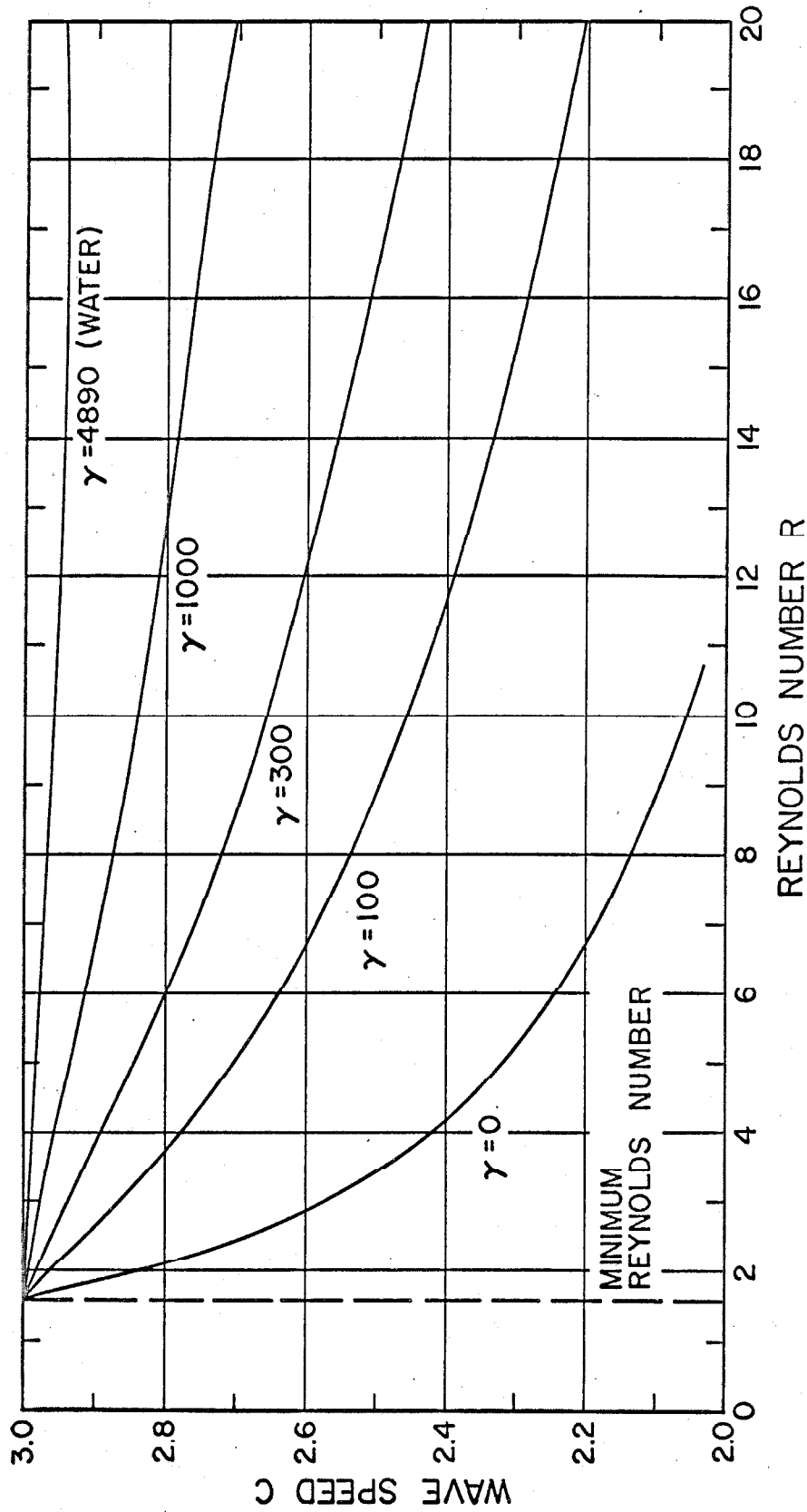


FIGURE 12: VARIATION OF WAVE SPEED WITH REYNOLDS NUMBER ON NEUTRAL-STABILITY CURVES FOR $\omega=30^\circ$

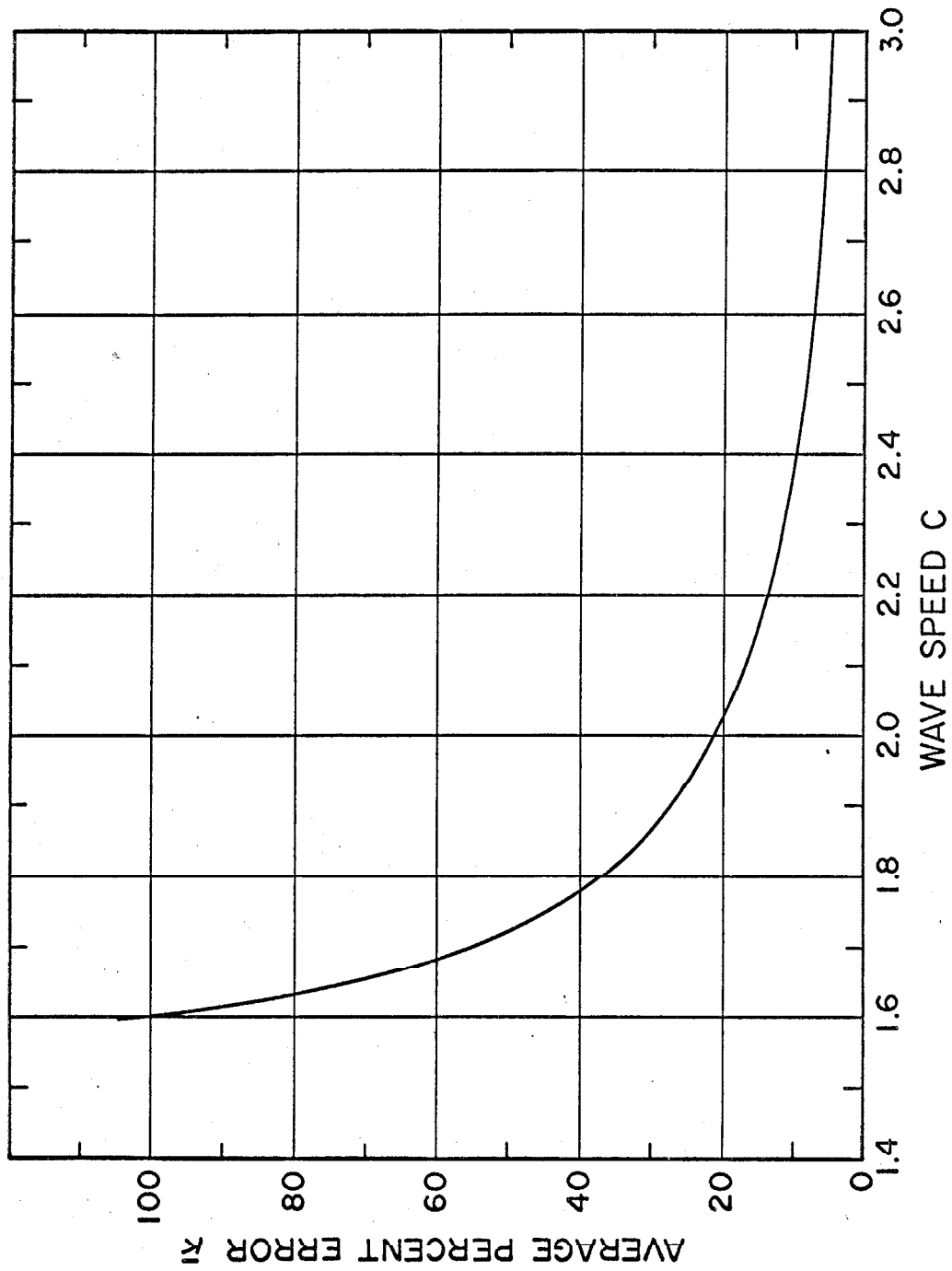


FIGURE 13: AVERAGE PERCENT ERROR IN THE QUANTITY $(c-U_0)$ RESULTING FROM ITS REPLACEMENT BY $(c-I)$

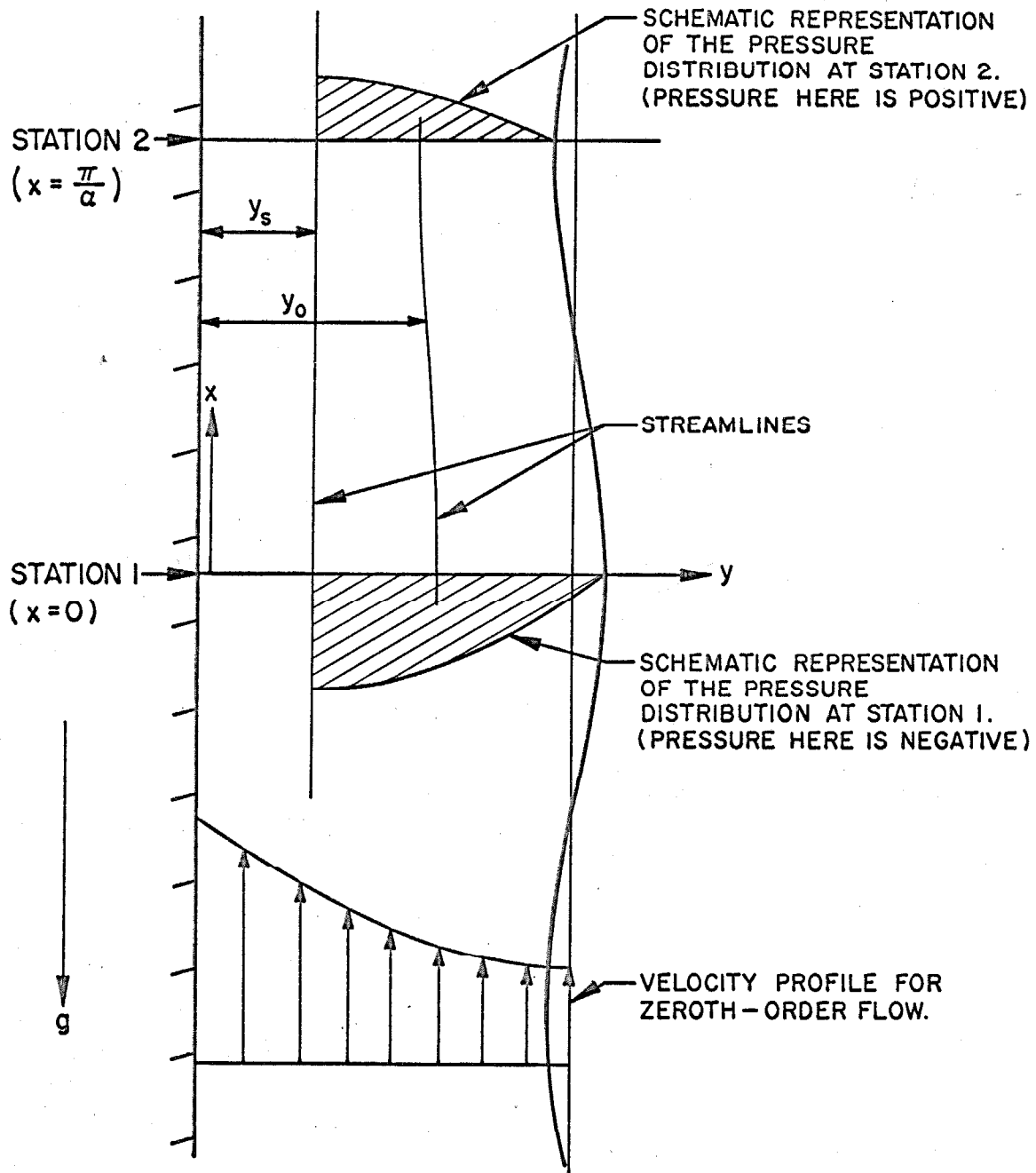


FIGURE 14: THE FLOW FIELD CONSIDERED IN SECTION 2.7

REFERENCES

1. Benjamin, T. B., "Wave Formation in Laminar Flow Down an Inclined Plane," J. Fluid Mech. 2 (1957), p. 554.
2. Binnie, A. M., "Experiments on the Onset of Wave Formation on a Film of Water Flowing Down a Vertical Plane," J. Fluid Mech. 2 (1957), p. 551.
3. Friedman, S. J. and Miller, C. O., "Liquid Films in the Viscous Flow Region," Industr. Engng. Chem. 33 (1941), p. 885.
4. Gluck, D. F., Gille, J. P., Zukoski, E. E., and Simkin, D. J., "Distortion of a Free Surface During Tank Discharge," J. Spacecraft and Rockets 3 (Nov. 1966), p. 1691.
5. Grimley, S. S., "Liquid Flow Conditions in Packed Towers," Trans. Inst. Chem. Engrs. 23 (1945), p. 228.
6. Heisenberg, W., "On the Stability of Laminar Flow," Proc. Int. Congr. Math. (1950), p. 292.
7. Jeffreys, H., "The Flow of Water in an Inclined Channel of Rectangular Section," Phil. Mag. (6) 49 (1925), p. 793.
8. Kapitza, P. L., J. Exp. Theor. Phys., U. S. S. R. 18 (1948), p. 3.
9. Kirkbride, C. S., "Heat Transfer by Condensing Vapors on Vertical Tubes," Industr. Engng. Chem. 26 (1934), p. 425.
10. Lamb, H., Hydrodynamics, 6th Edition (1945), Dover Publications, New York, p. 574.
11. Levich, V. G., Physico-Chemical Hydrodynamics, (1962) Prentice-Hall, New York, pp. 669-689.
12. Lighthill, M. J. and Whitham, G. B., "On Kinematic Waves," Proc. Roy. Soc. A, 229 (1955), p. 281.
13. Lin, C. C., "On the Stability of Two-dimensional Parallel Flows," Proc. Nat. Acad. Sci., Washington 30 (1944), p. 316.
14. Lin, C. C., The Theory of Hydrodynamic Stability (1955), Cambridge University Press, Oxford.
15. Saad, M. A. and Oliver, D. A., "Linearized Time Dependent Free Surface Flow in Rectangular and Cylindrical Tanks," Proc. 1964 Heat Transf. and Fl. Mech. Inst., Stanford University Press (1964), p. 81.

16. Shen, S. F., "Calculated Amplified Oscillations in Plane Poiseuille and Blasius Flows," J. Aero. Sci. 21 (1954), p. 62.
17. Squire, H. B., "On the Stability of the Three-dimensional Disturbances of Viscous Flow Between Parallel Walls," Proc. Roy. Soc. A, 142 (1933), p. 621.
18. Stoker, J. J., Water Waves (1957), Interscience Publishers, New York.
19. Yih, C. -S., "Stability of Parallel Laminar Flow with a Free Surface," Proc. 2nd U. S. Congr. Appl. Mech., Amer. Soc. Mech. Engrs. (1954), p. 623.
20. Yih, C. -S., "Stability of Liquid Flow Down an Inclined Plane," Phys. of Fl. 6 (1963), p. 321.
21. Yih, C. -S., Dynamics of Nonhomogeneous Fluids (1965), The MacMillan Co., New York, pp. 180-195.